ADVANCES IN MICROBIAL ECOLOGY, Vol. 9
Edited by K.C. Marshall
(Plenum Publishing Corporation, 1986)

Microelectrodes: Their Use in Microbial Ecology

NIELS PETER REVSBECH and
BO BARKER JØRGENSEN

1. Introduction

Among the fundamental goals of microbial ecology is the development of methods that will enable the identification and counting of the important microorganisms in nature, the determination of their physical and chemical microenvironment, and the analysis of their metabolic processes and interactions. Due to the small size of the organisms, much effort has been devoted to the development of high-resolution techniques for the observation and understanding of the world of bacteria on a microscale. Scanning and transmission electron microscopy and fluorescent staining, immunofluorescence and other techniques for light microscopy have been the most successful in terms of reaching a high spatial resolution. With respect to our understanding of the microbial microenvironments and of the nature of the microorganisms that carry out the measured metabolic activities, there is still a long way to go. Most chemical and radiotracer techniques in use today operate on a centimeter or at best on a millimeter scale and in most cases their results cannot be directly related to the relevant microorganisms. One notable exception to

NIELS PETER REVSBECH and BO BARKER JØRGENSEN • Institute of Ecology and Genetics, University of Aarhus, DK-8000 Aarhus C, Denmark.

this is the combined use of autoradiography and fluorescence microscopy on microbial communities.

High-resolution electrochemical techniques have been available, however, for many years without catching the attention of microbial ecologists. Simple, intracellular capillary electrodes with tip diameters of 1 μm or less have been used in neurophysiology since the 1950s for the study of action potentials and of ion transport over biological membranes. Ion-sensitive microelectrodes were later developed for the analysis of H^+, Na^+, K^+, and Ca^{2+}. These were either solid-state electrodes based on ion-selective glasses or liquid-membrane electrodes based on organic ion-exchangers. Again, the main use of the microelectrodes was in cell physiology, where they were applied mostly for intracellular analysis. In the 1960s polarographic microelectrodes with sensing tips of only a few micrometers appeared, which allowed measurements of oxygen in whole tissues and in cell cultures.

It may seem surprising that this important development of new analytical microtechniques, of obvious applicability to many problems in microbial ecology, had not reached this field many years ago. This is a classic example of the communication barrier between the different biological and technological disciplines, which has repeatedly delayed the introduction of new approaches.

In 1978, we started to use oxygen microelectrodes in our studies of the ecology and biogeochemistry of marine sediments and other microbial environments. The first aim was simply to analyze the microscale distribution of oxygen in order to identify the boundaries of aerobic and anaerobic metabolism in nature. We later developed microelectrode techniques to measure photosynthesis and respiration at high spatial and temporal resolution, and we also included pH and sulfide microelectrodes in our research.

Because so little work of relevance to microbial ecology had been done previously with these techniques, the present chapter necessarily is based heavily on our own work. The reader should therefore not anticipate a review of of a well-established research field, but rather a summary of our own limited experience with a new and fascinating methodology. Our motivation to write the review at this early stage has mostly been the interest we have experienced from many colleagues, who wish to introduce microelectrodes in their own research. We hope this chapter will be a help and inspiration to such new research. In the presentation we have included both a brief description of how to make and use microelectrodes as well as examples of different applications, which should give an impression of the technical problems involved and the many potential applications.

2. Microelectrodes and Measuring Equipment

2.1. Types of Microelectrodes

The four different types of microelectrodes used in microbial ecology are shown in Fig. 1. They comprise two types of oxygen microelectrodes, a sulfide microelectrode, and a pH microelectrode. Some publications describe measurements with "microelectrodes" that were several millimeters in diameter. We will not try to define an absolute size limit of a microelectrode, but an electrode having a diameter of more than 0.2 mm does not qualify as "micro." The term "electrode" is also used here for a combined sensor, such as the one shown in Figs. 1B and 2, which actually contains two electrodes, a sensing electrode and a reference electrode, both situated behind a polymer membrane. Two of the electrodes are commercially available: the cathode-type oxygen microelectrode (Diamond Electro-Tech, P.O. Box 2387, Ann Arbor, MI 48106) and the pH microelectrode (Microelectrodes, P.O. Box 365 Oak Hill Park, Londonderry, NH 03053). We have, however, always made our own microelectrodes, as described in the following sections.

2.1.1. Cathode-Type Oxygen Microelectrode

The type of oxygen microelectrode (Baumgärtl and Lübbers, 1983; Revsbech 1983) shown in Fig. 1A has been used in most published studies, but a slightly different design (Whalen *et al.*, 1967) also has been applied. Whalen's electrode is built around a core of Wood's metal instead of a platinum wire; Wood's metal is an alloy that melts at very low temperatures. The tip of Whalen's electrode is coated with gold, so that, electrochemically speaking, it is a tiny gold cathode, like the electrode shown in Fig. 1A. Both electrodes can be made with tip diameters of less than 1 μm.

Oxygen is sensed only at the very tip of the cathode-type oxygen microelectrode, where the membrane-covered gold surface is exposed to the medium. The microelectrode is charged at about -0.75 V versus a standard calomel reference electrode, and the current originating from the reduction of oxygen at the gold surface is proportional to the oxygen partial pressure in the surrounding medium. Because of the small size of the electrode tip, diffusion is fast relative to convective transport (Purcell, 1977; Crank, 1983) in supplying oxygen to the reducing metal surface. Convection by stirring therefore gives only a 1–5% increase in current compared to the current in stagnant medium. Because of the small size and short diffusion path, the 90% response time can be less than 0.2 sec.

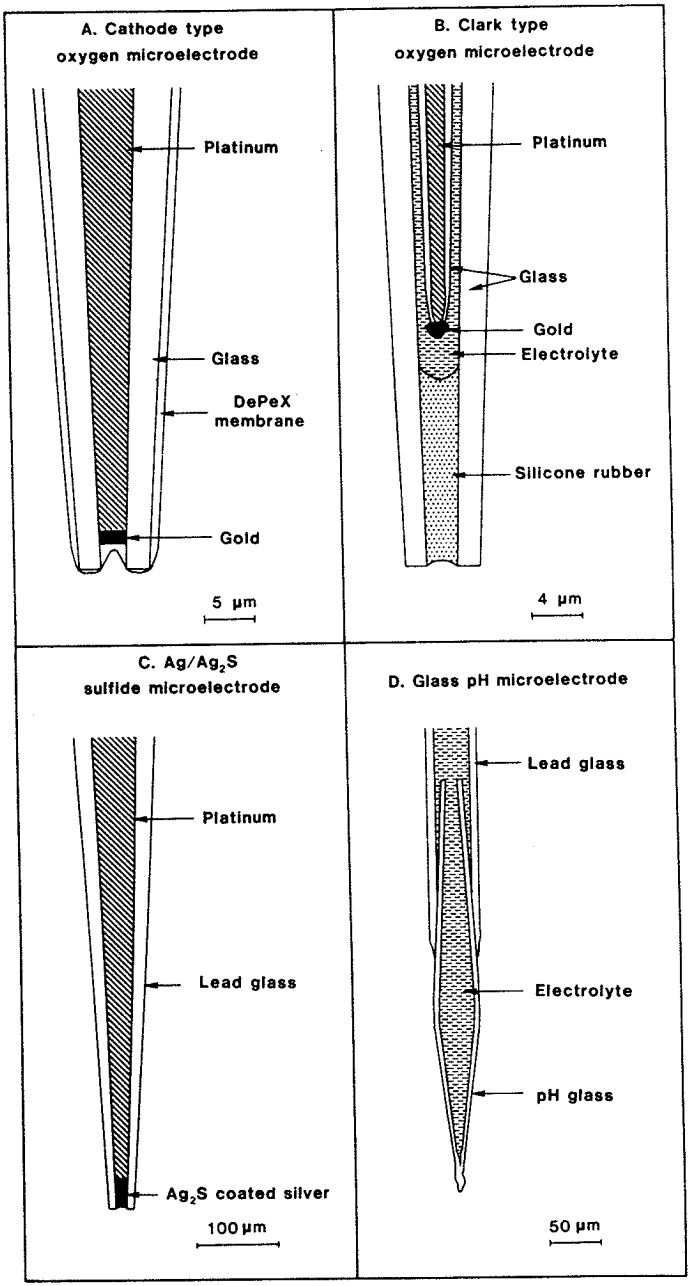

Figure 1. Sensing tips of the four types of microelectrodes that have been used in microbial ecology. [Redrawn from Revsbech (1983).]

The response time can be measured by quickly introducing the electrode from air into deoxygenated water. Electrical contact between the cathode and the reference electrode while the microelectrode is in water-saturated air can be maintained via the wet microelectrode surface.

The oxygen microelectrode can be made to withstand high hydrostatic pressures by filling the air space within the shaft with oil (C. E. Reimers, unpublished data). These pressure resistant electrodes are now being used for *in situ* measurement of oxygen microprofiles in pelagic sediments at 4000 m water depth.

A coaxial design of the electrode shown in Fig. 1A has been described by Baumgärtl and Lübbers (1983). The glass shaft of their electrode is coated with multiple thin layers, the outermost consisting of silver. The silver layer shields the platinum wire inside the microelectrode from electrical noise, and at the same time the chlorinated silver layer serves as a reference electrode. Such an external reference electrode may, however, be affected by some of the ions (e.g., sulfide) in the medium, and this will prevent its application in many environments. The greatest problems in the construction and use of the oxygen microelectrodes described above are associated with the membrane. The membrane must allow oxygen to pass through, and at the same time it must be electrically conducting; i.e., it must be permeable to at least some ions. Both Mg^{2+} and Ca^{2+} poison the electrodes, most probably by precipitation of hydroxides and carbonates on the gold surface (Baumgärtl and Lübbers, 1983), which becomes alkaline during the reduction of oxygen to OH^-. Dissolved organic matter may also poison the electrode. The membrane should therefore not be permeable to these poisoning substances. It is difficult to make a sufficiently thin membrane that at the same time will prevent large, double-charged cations to pass through and still be permeable to oxygen and small ions such as K^+ and Na^+. The membrane often has to be applied several times before a satisfactory result is obtained (Revsbech 1983). Because of these problems with the membrane, the signal from this type of oxygen microelectrode is seldom very stable when used in natural media. The electrodes described by Whalen *et al.* (1967) can be made with a very deep recess at the tip. The deep recess improves the stability of the electrode when used in animal or human tissue (P. Nair, personal communication), but it is not known whether this will be the case also in other media. According to P. Nair, a membrane should not even be necessary when the recess is sufficiently deep.

It is our experience that a usable response of the oxygen microelectrodes described above cannot be obtained in media that are both high in Mg^{2+} or Ca^{2+} and low in Na^+ and K^+. The instability is expressed both as a slow drift and as an increased sensitivity to oxygen after periods at low oxygen tensions. The increase in sensitivity after periods at low oxy-

gen is probably due to dissolution of precipitates at the gold surface during these less OH^--producing conditions.

The oxygen microelectrodes are poisoned by sulfide (Revsbech *et al.*, 1980b), but after the first exposure, the effect of sulfide is small. Electrodes for use in media where they may encounter hydrogen sulfide should therefore be poisoned before use. A "conditioning" of the electrode in sediment before using it to record oxygen profiles within the sediment was recommended by Reimers *et al.* (1984). The conditioning also improved the stability when no hydrogen sulfide was present.

2.1.2. Clark Microelectrode

The problems with the membrane of the cathode-type oxygen microelectrodes described above were solved (Revsbech and Ward 1983) by developing a combined microsensor (Figs. 1B and 2) that is a small version of the conventional Clark electrode (Clark *et al.*, 1953). In this microsensor, the cathode is situated behind an electrically insulating membrane of silicone rubber (Fig. 1B), which is extremely permeable to

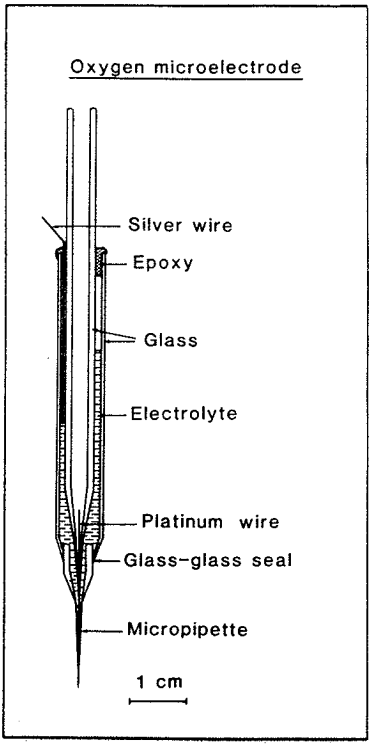

Figure 2. Oxygen microelectrode of the Clark type. The electrode tip is shown in Fig. 1B. [From Revsbech and Ward (1983).]

oxygen (Shiver, 1969). The cathode is bathed in an electrolyte solution of 1 M KCl into which a Ag/AgCl reference electrode (Fig. 2) is immersed. The electrolyte solution also serves as an electrical shielding of the cathode. This electrode has a response time comparable to the cathode-type oxygen microelectrode shown in Fig. 1A, and it is also insensitive to stirring. The signal from the electrode is much more stable, however. The current drift is often less than 2%/hr even when used in natural media containing various salts and dissolved organic compounds. The linearity of the signal versus oxygen tension is 100% for almost all electrodes. The tip diameter has been made smaller than 2 μm, but it is also possible to make thicker and much sturdier electrodes for use in systems like soils (Sexstone *et al.*, 1985) and coarse sediments, which require mechanical strength.

2.1.3. Sulfide Microelectrode

The sulfide microelectrode (Revsbech *et al.*, 1983) shown in Fig. 1C is a small Ag/Ag_2S electrode. The problems associated with the use of sulfide electrodes are discussed by Berner (1962) and Guterman and Ben-Yaakov (1983). The chemical species actually being sensed by the electrode is S^{2-}ion, the concentration of which is dependent on both the total concentration of dissolved sulfide and pH. Knowledge about the exact pH at the point being analyzed is therefore essential for the interpretation of the readings obtained using the sulfide microelectrode. Theoretical calculations of the total amount of dissolved sulfide from electrode potential and pH are not sufficiently accurate, and in practice it is always necessary to calibrate the electrode. There are, however, often problems with drift of the potential, so that recalibration may be necessary. Due to the high pK of the HS^-–S^{2-} pair (11.96), the detection limit for total sulfide is not very low, about 10 μM at pH 7–8, and the calibration curve of electrode potential versus log(S^{2-}) is nonlinear at concentrations below 100 μM total sulfide.

2.1.4. pH Microelectrode

The pH microelectrode shown in Fig. 1D is a small version of the large, commercial glass pH electrodes. The electrode shown in Fig. 1D is relatively sturdy and it is also easy to make. Various other designs of pH microelectrodes are possible (Thomas, 1978), and tip diameters of less than 1 μm can be obtained. Some types of pH microelectrodes have the pH- sensitive glass cone within a recess at the electrode tip, whereas others are made with a liquid pH-sensitive membrane (Ammann *et al.*, 1981). The electrodes with a liquid membrane have inferior specificity to

hydrogen ions as compared to the glass electrodes, and they also have a shorter lifetime. They are, however, relatively easy to construct and can be made with tip diameters of less than 1 μm.

Calibration of the pH microelectrodes should be carried out in buffers of similar ionic composition as the media in which they are used, as considerable interference by other ions, especially Na^+, may occur. Old and "overhydrated" electrodes were found to give a potential almost one pH unit off the actual value when first calibrated in standard pH buffers and afterward used in a seawater salt brine of 80% salinity (N. P. Revsbech, unpublished data). Correctly hydrated electrodes (Section 2.2.4) gave a negligible error. Good pH microelectrodes with correctly hydrated pH-glass have linear calibration curves in the range from pH 4 to 10 with slopes of 57–59 mV/pH unit when calibrated at room temperature. Excessively hydrated electrodes may have slopes of less than 50 mV/pH unit.

2.2. Construction of Microelectrodes

A very good introduction to working with glass in small dimensions and to the construction of various ion-selective microelectrodes is given by Thomas (1978). It is not possible to outline all the details for the construction of microelectrodes here, but we will give a short description of how the electrodes shown in Fig. 1 are made.

The equipment necessary for making the electrodes is quite simple, the most expensive parts being two micromanipulators ($400–600 each), a light microscope with the ability to give a good resolution at 100× and 400× magnification, and a dissection microscope with magnifications adjustable from about 10× to 50×. Physiologists often use electrode pullers to make the very delicate microelectrodes for intracellular use, but we have never found such equipment necessary or advantageous for the construction of our electrodes.

2.2.1. Construction of Cathode-Type Oxygen Microelectrode

The oxygen microelectrode shown in Fig. 1A is made around a core of tapered platinum wire (99.99% purity, annealed/slightly hard-drawn condition, 0.1-mm thermocouple wire from Engelhard Industries, Surrey, U.K.). The platinum wire is finely tapered by etching in a 90% saturated KCN solution while 2–7 V ac is applied. The other electrode immersed into the KCN solution to complete the circuit consists of a graphite rod from a pencil. A voltage of 7 V is applied while 1 cm of the wire is immersed in the KCN solution. The current is reduced to 2 V when the 1-cm tip has almost disappeared, and the etching is continued for a few

seconds. The initially high voltage during etching creates a smooth surface on the platinum, but the tip becomes blunt. Etching at low voltage tends to create cavities in the platinum, and it should therefore only be applied for a short period, but it is essential for the creation of a thin tip.

The etched platinum wires are cleaned in water, sulfuric acid, and alcohol, and are then inserted into precleaned soda-lime capillaries (AR-glas, Glaswerk Wertheim, West Germany). These capillaries should be thin-walled, but the internal diameter should be at least 0.25 mm. The platinum is coated with glass by hanging the capillary vertically through an electrically heated nichrome loop (Fig. 3). Melting of the glass should start around the nonetched platinum wire, about 1 cm from the etched part. When the glass melts, gravity pulls the platinum wire through the melting zone, and a thin glass coating is produced. It is often necessary to attach a 2-g weight to the electrode shaft to obtain a sufficient pull by gravity.

The tip of the platinum is totally covered with glass after a successful melting as described above. The very tip of the platinum must therefore be exposed by grinding off excess glass on a rotating disc covered with 0.25-μm grain size diamond paste. For electrodes of the type shown in

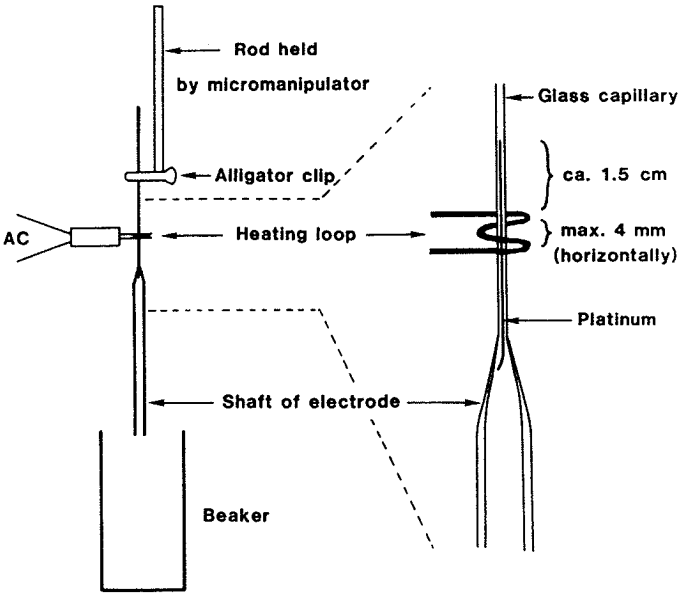

Figure 3. Left: Coating of platinum wire with glass. When the loop is heated, the glass capillary inside the loop melts, and the glass shaft falls down into the beaker. Right: Position of platinum wire relative to heating loop before heat is applied.

Fig. 1A, it is advisory to proceed with the grinding until a tip diameter of 5–9 μm is obtained. After grinding, the platinum at the tip should be etched briefly in KCN so that a 5–10 μm-long recess is formed.

The platinum in the recess is coated with gold by electroplating as described by Baumgärtl and Lübbers (1983). The gold-plating solution [5% $KAu(CN)_2$ in water] may be contained in a thin capillary so that the process can be observed under the microscope. The electrode should soak in water for 1 day after the electroplating. After this, the tip of the electrode is coated with a polymer membrane as described by Revsbech (1983). The electrode is ready for a test of performance after hydration of the membrane for 1 day.

2.2.2. Construction of Clark Microelectrode

The cathode of the Clark microelectrode shown in Figs. 1B and 2 is made largely as described above for the cathode-type oxygen microelectrode. The platinum wire must, however, be etched to a longer and thinner tip, since the cathode is then easier to fit into an outer casing. Furthermore, a recess is not etched at the cathode tip before gold plating, and a membrane is not applied on the cathode.

The tip of the outer casing is shaped in several steps by gravitational pull in electrically heated metal loops as shown in Fig. 3. A small loop made of 25-μm-thick platinum wire (also used for making pH microelectrodes as shown in Fig. 4) is used for the final step. The membrane of silicone rubber is applied by inserting the tip into uncured silicone rubber (Silastic, Medical Adhesive type A, Dow Corning, Midland, MI 48640). The membrane enters the tip by capillary suction, and the tip should be withdrawn from the silicone rubber when 10–20 μm of the capillary is filled. The cathode is inserted into the outer casing using a micromanipulator, and a partial seal of epoxy is applied between cathode and casing. After the epoxy and silicone have cured for 1 day, the electrolyte consisting of 1 M KCl saturated with thymole is injected, a chlorinated silver wire is inserted, and the electrode is ready for use.

2.2.3. Construction of Sulfide Microelectrode

The Ag/Ag_2S sulfide microelectrode is constructed by procedures rather similar to the ones described above for the cathode-type oxygen microelectrode. The soda-lime glass is, however, substituted with the electrically more insulating lead glass (e.g., 28% PbO Bleiglas, no. 8095, Schott Glaswerke, Mainz, West Germany). The silver layer is applied by electroplating (Revsbech *et al.*, 1983), and the electrode is immersed into 0.1 M ammonium sulfide solution to form the Ag_2S coating.

2.2.4. Construction of pH Microelectrode

The pH microelectrode shown in Fig. 1D is made by a simpler procedure than that outlined by Thomas (1978). It is constructed from pH-sensitive glass [Corning 0150, suppliers listed by Thomas (1978)] and lead glass. The pH-glass is drawn in a soft flame to 0.2- to 0.3-mm-thick capillaries, which are then pulled by gravity in an electrically heated metal loop as described above and shown in Fig. 3. The weight attached to the capillary should be large ~10 g, and the heat applied should be low. The capillary will then form a conical tip when it falls down. The extreme tip is broken off so that a 5- to 10-μm-wide opening is formed.

The lead glass used for the shaft of the electrode is pulled in a flame so that a capillary with a diameter of 0.5–1.0 mm is formed. This capillary is pulled by gravity as described above for the pH-sensitive glass, but here the temperature of the heating loop should be high and the weight attached to the capillary only 2 g. The lead glass will then form a very long, 20- to 50-μm-wide capillary. The thin glass capillary is broken about 1 cm from the shoulder to the thicker capillary. A clean cut is preferable, and this can be obtained by scraping the capillary with silicon carbide crystals before breaking.

The lead glass capillary is positioned, tip upward, on a small adjustable stand. The pH-glass cone is now introduced into the lead glass capillary using a micromanipulator. After making a glass–glass seal (Fig. 4), the small stand is lowered so that the lead glass is hanging in the pH-glass capillary. The pH-sensitive cone is now made by heating the pH-glass just above the fusion zone. Finally, the tip of the electrode is closed by positioning the very hot platinum heating loop just above the tip. The filling of the electrode with electrolyte and the hydration at high temperatures are described by Thomas (1978). Our electrodes are normally allowed to hydrate for 3 or 4 days at 70°C.

2.3. Measuring Equipment

The impedances in the microelectrode measuring circuits are about 10^{-10} Ω for the oxygen microelectrodes and between 10^{-7} and 10^{-11} Ω for the pH microelectrodes, depending on the size of the individual electrode, the degree of hydration, etc. Because of the high impedances, the signals from the electrodes are very sensitive to electromagnetic interference. The measuring circuits used should thus be designed to minimize such electrical noise, and they should also be able to amplify the small signals so that accurate readings can be obtained. Requirements of the measuring circuit other than stability and high sensitivity may, however,

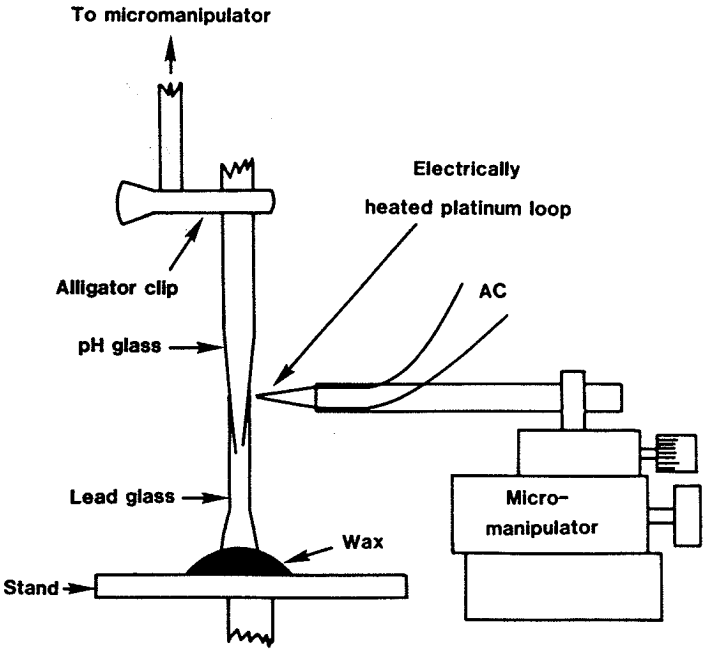

Figure 4. Fusion of pH and lead glasses for a pH microelectrode. The sizes of capillaries, lead glass shaft, etc., are not drawn to the same scale.

be important for optimal use of the microelectrodes in different ecological applications.

2.3.1. Measuring Circuits

A setup for measuring oxygen in a sediment core is shown schematically in Fig. 5. The microelectrode is held by a micromanipulator, which can be used to introduce the microelectrode tip into the substratum with a depth resolution of better than 10 μm. A micromanipulator with a motordrive (e.g., Mertzheuser, Steindorf/Wetzlar, West Germany) can be recommended, since it is difficult to operate the micromanipulator without causing uncontrolled vibration of the microelectrode tip. All cables conducting the primary signal must be of "low-noise" quality (with additional graphite shielding inside the copper shield) to minimize electrical noise associated with movement of the cables. The cables should be mounted on the microelectrodes in such a way that the contact between the inner conductor of the cable and the signal conducting metal wire of the microelectrode can be kept completely dry. The cable can be mounted

(Fig. 6) on the combined oxygen microelectrode as shown in Fig. 1B. An electrode holder made of Plexiglas (Revsbech, 1983) is, however, more convenient for laboratory use. Desiccant in the electrode holder is a necessity, since even moderate air humidity may cause erratic signals originating from currents creeping along the humid glass surfaces. The current in the circuit must be measured by a very sensitive ammeter with a range down to 1 pA (10^{-12} A). The amplified signal can then be recorded on a strip-chart recorder. The tracing shown in Fig. 5 is the actual tracing from the measurement of an oxygen profile in a dark-incubated, sandy sediment. The time it took to obtain a stable reading when the electrode tip was moved to a new layer (Fig. 5) was caused by the response time of the electrode, disturbance of the oxygen gradients when sand grains moved during the advancement of the electrode, and the time it actually took to move the electrode. The oxygen profile calculated from the tracing is shown to the right in Fig. 5.

In the measuring circuits for sulfide and pH, the picoammeter and voltage source in the oxygen microelectrode circuit are substituted by a high-impedance voltmeter. The cable between the voltmeter and electrode should be kept as short as possible.

Under conditions where electrical noise originating from extensive

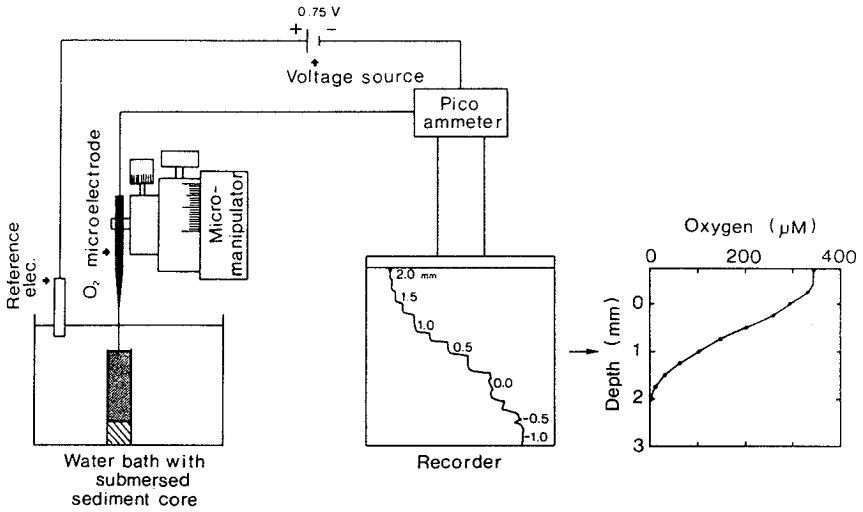

Figure 5. Simple circuit for measurement with oxygen microelectrodes. The microelectrode tip was first positioned in the water 1 mm above the sediment. It was then advanced downward into the sediment at increments of 0.25 mm. The current in the circuit at various depths was recorded on a strip-chart recorder. The oxygen profile to the right was calculated from this tracing.

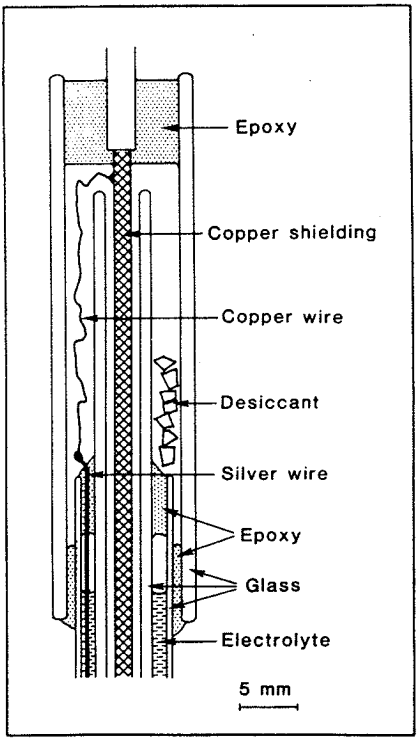

Figure 6. Connection of shielded cable with oxygen microelectrode of the type shown in Fig. 2. Electrical contact with the silver wire serving as reference electrode was made through the copper shielding of the cable. Electrical connection between the platinum wire in the tip region of the electrode and the inner conductor of the cable was made by simple contact. [From Revsbech and Ward (1983).]

movement of the cables becomes unacceptable, e.g., on board vibrating ships or under windy conditions in the field, it may be an advantage to build an amplifier into the electrode holder itself. Such devices have been described for both oxygen microelectrodes (Reimers *et al.*, 1984) and pH microelectrodes (Thomas 1978). Reimers and coworkers found that the electrical noise level on board ships could be reduced ten-fold in this way. Also, the positioning of the electrode within the substratum may be poorly defined when the vibration level is high. Especially when measuring with very small pH microelectrodes, the slow response caused by the capacity of an even moderate length of shielded cable may be unacceptable, and this problem is also solved by placing an amplifier in the electrode holder.

All the equipment for experimental work with microelectrodes can be made portable, and it is thus possible to measure microprofiles of oxygen, sulfide, and pH in the field. There are no serious problems in doing this when the substratum is mechnically stable, when the sun is shining, and when the air humidity is low. Useful data have been obtained by field work in Solar Lake, Sinai (Jørgensen *et al.*, 1979) and in hot springs of

Yellowstone National Park (Revsbech and Ward, 1983, 1984a,b). It has even been possible to do *in situ* experiments at a water depth of several meters, where the micromanipulator had to be operated by a diver (Lindeboom and Sandee, 1984), and it is expected that measurements will soon be done in the deep sea with the microelectrodes mounted on a free-falling vehicle or operated from a submersible. Field work in coastal sediments with the delicate electrodes may, however, also be a frustrating experience, especially due to the many snails, crabs, fish, etc., which always seem determined to approach and break the microelectrodes.

2.3.2. Computerized Data Collection

The circuit shown in Fig. 5 is able to record the data for later analysis, but for many applications it is advantageous to feed the signal from the picoammeter directly into a computer. We have often found that simple data handling and calculation took much more time than the actual measurements. An example of a custom-built, computer-based data collection system we have developed is shown in Fig. 7. The signal from the picoammeter is fed into a 12-bit analog-to-digital converter, which transforms the signal into a figure between 0 and 4095. Light intensity and other analog signals also may be fed into the converter. The digital signals from the converter are fed into a data collection unit, and the pulses from a stepper motor on the micromanipulator are also counted by this unit. In this way, coupled data points of electrode current and depth are received. (A micromanipulator equipped with stepper motor is sold by Fairlight Scientific & Industrial Equipment, Postbus 4055, 3006 AB Rotterdam, The Netherlands.) The data collection unit is in fact a small, independent computer, which sorts out the essential sets of information from the large amounts of data entering through the input channels. The

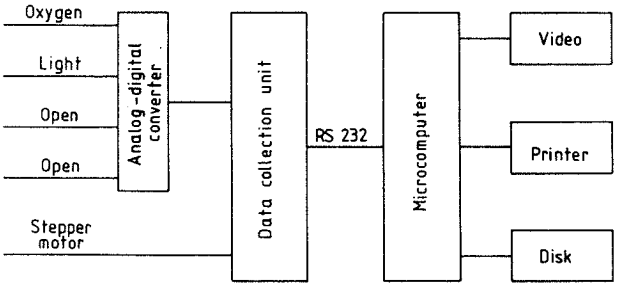

Figure 7. Schematic diagram of computerized data collection from microelectrode circuit. The positioning of the motor-driven micromanipulator and other parameters, such as light, can also be read into the computer.

data, which are transmitted further to the microcomputer via a serial RS 232 interface, may for example, only be transmitted for every 0.1-mm depth interval or for every 0.1 sec. The programs based upon which the data collection is performed are contained in an ROM (read only memory) chip built into the data collection unit. The microcomputer performs calculations on the data simultaneously with the collection of new data. Both data and results of calculations are stored on "floppy disks." The results of the calculations can be displayed on a video monitor and printed out on a dot-matrix printer. Another data collection system based on a programmable calculator (HP41C from Hewlett Packard) has been developed for the measurement of *in situ* oxygen microprofiles in deep-sea sediments (C. E. Reimers, unpublished results), and in connection with a datalogger (3421A from Hewlett Packard), for photosynthesis measurements (B. B. Jørgensen, unpublished results).

3. Microelectrode Applications

Microelectrode studies have been done in a wide variety of environments and microbial communities, mostly in sediments, and microbial mats. Because of the large amount of data available for sedimentary ecosystems, examples of microelectrode measurements in sediments will be treated first, and data obtained in sediments will be used to illustrate the general principles, applications, and problems associated with the use of microelectrodes in microbial ecology.

3.1. Oxygen Distribution in the Microenvironment

3.1.1. Oxic versus Oxidized Conditions

It is of fundamental importance for the understanding of microbial processes to know the environmental conditions at the site where the processes occur. It is especially important to know whether oxygen is present or not. Before the introduction of oxygen microelectrodes in ecological research, the oxygenated surface layer in sediments was often assumed to be identical to the brown, oxidized surface layer. The brown surface layer is virtually identical with the layer having a positive redox potential as read with a redox electrode (Fenchel 1969). Profiles of oxygen and redox typical of coastal, sandy sediments (Revsbech *et al.*, 1980a,b) are shown in Fig. 8A. The oxic zone shown in Fig. 8A was only 2 mm thick, whereas a positive redox potential was found down to a depth of 3.5 cm. The oxic–anoxic interface could not be distinguished on the redox profile, and substances other than molecular oxygen must consequently be able to

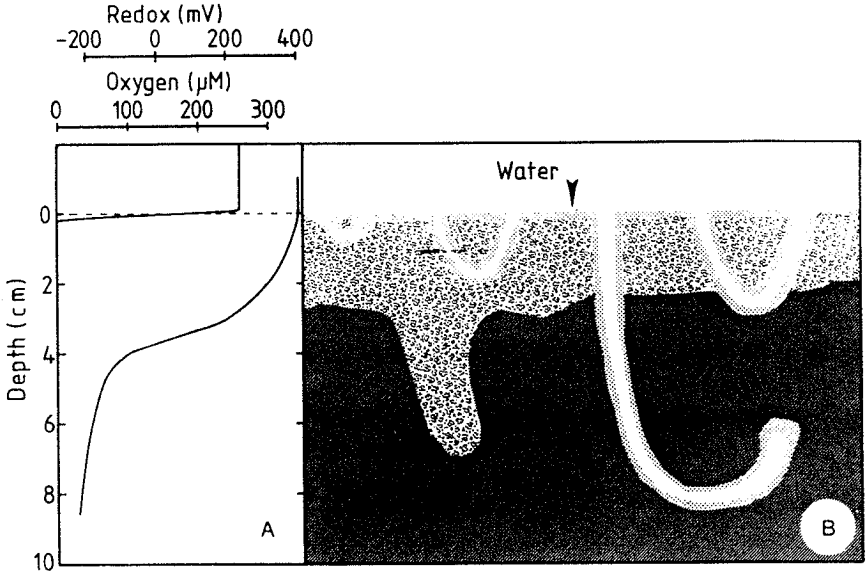

Figure 8. Oxic versus oxidized conditions. (A) Oxygen and redox profiles from the sediment shown in (B) (measured at point marked with arrow). Oxygen was found only in the uppermost 2 mm of the sediment and in the immediate vicinity of animal burrows (light dotted areas). The periodic introduction of oxygen into parts of the sediment caused by the activity of the infauna kept an ~3-cm-thick surface layer oxidized ("grainy" area) and even deep in the generally reduced sediment (dark area), deeply burrowing infauna caused local oxic and/or oxidizing conditions.

give the sediment a high, positive redox potential. This is not surprising, as the sediments often contain considerable amounts of iron and manganese, which in their oxidized forms can be responsible for such positive redox potentials. It is more difficult to understand, however, how such predominantly insoluble compounds are kept oxidized without oxygen being present. Oxidized manganese and iron compounds are continuously being reduced by the metabolic activity of some bacteria (Jones *et al.*, 1983), and they are also reduced by hydrogen sulfide formed by sulfate-reducing bacteria. It is likely (Revsbech *et al.*, 1980a) that the major part of the reoxidation at any given sediment location does not occur continuously, but occurs by local or periodic events. These events may be reworking by infauna, or introduction of oxygen due to impact of currents and waves during storms. The reworking of the sediment by infauna ["bioturbation" (Aller, 1977)] is often able to keep a relatively thick surface layer oxidized (Edwards, 1958; Davis, 1974). Localized strongly reducing conditions may be found close to the surface in such sediments if by chance for an extended period of time no animal has oxygenated

From the initial decrease in oxygen after a light–dark shift (Fig. 24), a photosynthetic rate of 410 μM/min could be calculated. Measurements in other polyps showed photosynthesis rates of up to 3300 μM/min. Due to the complex anatomy of corals and the annular positioning of their symbiont population, it is difficult to calculate the quantitative importance of this symbiotic photosynthesis for the energy metabolism of the whole coral.

Planktonic foraminifera, however, with their small size and spherical symmetry, seem to be ideal systems for such a quantitative analysis. Spinose, symbiont-bearing foraminifera are common in the plankton of tropical oceans (Be and Tolderlund, 1971). These 0.1- to 1-mm protozoa build multichambered shells, which house the protoplast with its multitude of intracellular zooxanthellae (Anderson and Be, 1976). The symbionts are actively spread out by the host around the shell during the daytime. They are imbedded in pseudopodia, which glide out along the radial spines. By carefully approaching the animal between the spines with an oxygen or pH microelectrode it was possible to study the chemical microenvironment of the organisms as well as their metabolic activity. An impression of this microenvironment is given in Fig. 25.

The dimensions of the foraminifer *Globigerinoides sacculifer* with its surrounding halo of intracellular symbionts are shown in Fig. 25A. As the oxygen microelectrode radially approached the shell in the light, the oxygen concentration was found to increase steeply to 2.5 times the ambient air saturation of seawater (Fig. 25B). Thus, the total symbiotic system had a high net photosynthesis. The corresponding decrease of oxygen in the dark reflected the combined respiratory activity of host and symbionts. Rapid light–dark shifts showed that the oxygen pool in the microenvironment was even more dynamic than shown for the coral (Fig. 25C). With a photosynthesis rate of 2700 μM/min at the shell surface, as calculated from the initial oxygen decrease in the dark, the mean residence time of oxygen in the light was only 12 sec. This shows that the oxygen environment of the animal changes sufficiently rapidly to follow closely fluctuations in light intensity due, for example, to clouds passing the sun. In addition, the pH of the seawater around the foraminifer changed according to the intensive CO_2 uptake or release in the light or in the dark, respectively (Fig. 25D).

With the oxygen microelectrode it was possible to map the radial distribution of photosynthesis around the shell as well as to penetrate carefully into the shell (Fig. 26). The measurements were taken at 50-μm increments, each measurement being representative of a 50-μm-thick spherical shell concentrically surrounding the host. Connected values of photosynthesis and spherical shell volumes were then multiplied and summed to yield the total gross photosynthesis of the symbiotic system,

and oxidized that particular area. The concept of bioturbation as an electron carrier in sediments is illustrated in Fig. 8B. The oxidized sediment layer may constitute an ecologically important redox buffer (Board, 1976; Jørgensen, 1977) in the case of periodic oxygen deficiency of the overlying water.

3.1.2. Factors Affecting the Oxygen Distribution in Sediment

The very superficial penetration of oxygen into the sediments shown in Figs. 5 and 8 is typical for most shallow water sediments (Sørensen *et al.*, 1979; Revsbech *et al.*, 1980a; 1980b; Lindeboom and Sandee, 1984). The penetration of oxygen is governed by the rate of diffusional supply of oxygen to the sediment and by the rate of net oxygen consumption per unit volume of sediment. Assuming a uniform depth distribution of oxygen consumption, one can calculate the depth of penetration h of oxygen into a sediment from (Revsbech *et al.*, 1980a)

$$h = 2D_sC_0\phi/J \tag{1}$$

where D_s is the apparent diffusion coefficient of oxygen in the sediment, ϕ is the porosity, C_0 is the oxygen concentration at the sediment surface, and J is the oxygen consumption per unit area of the sediment surface. The inverse relationship between oxygen penetration and oxygen consumption described by Eq. (1) is in accordance with the thick oxic surface layers in deep sea sediments where the oxygen consumption is low (Smith and Baldwin, 1984; Smith and Hinga 1983). Deep oxygen penetrations have been measured by microelectrodes (Reimers *et al.*, 1984) and by gas chromatography [$>$60 cm measured by Murray and Grundmanis (1980); $>$100 cm measured by Sørensen (1984)] in cores collected in the deep sea.

Any impact causing a change of the variables on the right side of Eq. (1) would result in a different oxygen penetration. Three oxygen profiles measured in the same sediment core collected from a shallow, sandy area are illustrated in Fig. 9. The profile shown in Fig. 9A was recorded while a water current of 5 cm/sec was maintained above the sediment surface. The diffusive boundary layer (Jørgensen and Revsbech, 1985) above the sediment was 0.2 mm thick and caused a decrease in the concentration of oxygen from 252 μM in the overlying water to 228 μM at the sediment surface. The stirring of the water had been stopped for 1.5 hr when the profile shown in Fig. 9B was measured. The lack of stirring caused a thickening of the diffusive boundary layer above the sediment to about 1 mm. The thicker diffusional barrier caused a reduction of the oxygen con-

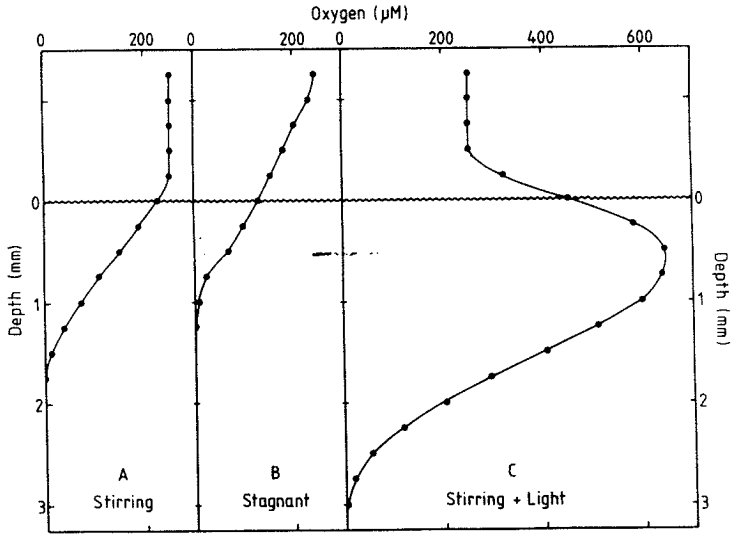

Figure 9. Oxygen profiles in a shallow, sandy sediment under various environmental conditions. (A) Current rate of ~5 cm/sec above the sediment, (B) stagnant overlying water, (C) as in (A), but with photosynthetic oxygen production by the benthic microbiota caused by illumination at 200 μEinst/m^2 per sec. Temperature at 22°C.

centration at the sediment surface to 130 μM and a reduction of the oxygen penetration from 1.7 to 1.2 mm.

The oxygen profile after an illumination period of 1.5 hr is shown in Fig. 9C. The photosynthesis in the surface layers caused both very high oxygen concentrations and an increase in the thickness of the oxic zone to 3.0 mm.

3.1.3. Diffusive Boundary Layers

The diffusive boundary layers described in Section 3.1.2 exist around all surfaces covered by liquids. The diffusive boundary layers are created by viscous forces, which cause a thin film of water to "stick" to the surface. The water in these films does not participate in the general circulation. Within the diffusive boundary layer, the transport of solutes occurs by molecular diffusion, whereas eddy diffusion is insignifcant as a transport mechanism (Santschi *et al.*, 1983). The diffusive boundary layer thus constitutes a diffusional barrier, which may limit the exchange of dissolved molecules between the surface and the bulk of the liquid. The boundary layers are especially important for the exchange of nutrients between microbial communities and their aquatic environment. Oxygen

microelectrodes are ideal tools for the study of diffusive boundary layers (Jørgensen and Revsbech, 1985). The electrodes give information about both the thickness of the boundary layer and the extent to which it is a stable diffusive layer, i.e., whether the oxygen profile through the boundary layer can be explained by steady-state molecular diffusion. We use the term *true diffusive boundary layer* for the layer in which the linear oxygen profile can be explained by pure molecular diffusion, and the term *effective diffusive boundary layer* as explained in Fig. 10 (cf. Jørgensen and Revsbech, 1985).

The diffusive boundary layer covers the sea bottom as a thin blanket as shown in Fig. 11. The bulk water flow above the sediment was 5–10 cm/sec when we measured the oxygen profiles. The diffusive boundary layer above relatively smooth surfaces is about 0.1–0.2 mm thick at such current rates, whereas it is about 1 mm thick in stagnant water. Such thick diffusive boundary layers must cover the entire deep sea floor (Baudreau and Guinasso, 1982; Wimbush, 1976), where the currents are very slow. Small protrusions from the sediment surface are able to penetrate through most of the boundary layer, as its thickness is not only dependent on the current velocity above the substratum, but also on the size of the

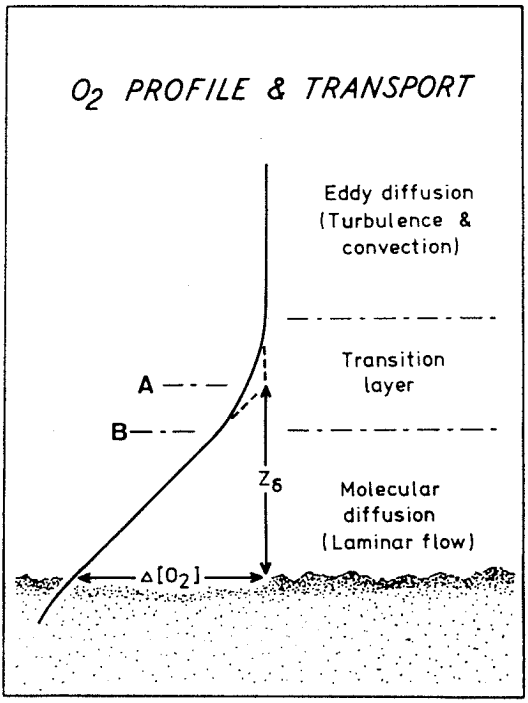

Figure 10. The diffusive boundary layer at the sediment–water interface as determined by the oxygen microgradients. Here *A* and *B* define the outer limits of the effective diffusive boundary layer and the true diffusive boundary layer, respectively. The thickness of the effective diffusive boundary layer is marked Z_δ. [From Jørgensen and Revsbech (1985).]

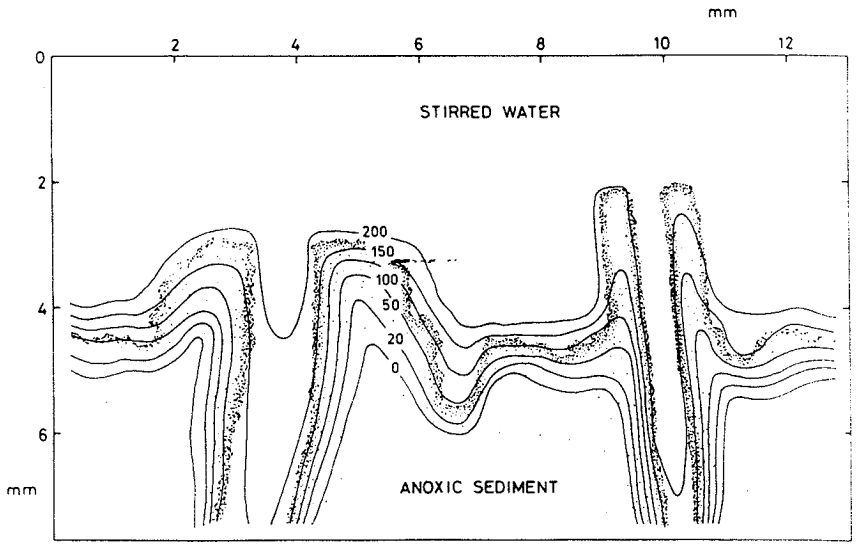

Figure 11. Isopleths of oxygen in a shallow sediment inhabited by two small polychaete worms. The isopleths show how the diffusive boundary layer created an oxygen gradient just above the sediment surface, and how this oxygen gradient followed the topography of the sediment. [From Jørgensen and Revsbech (1985).]

object. Small objects that protrude like the worm tubes shown in Fig. 11 thus reach into more oxic water than found at the normal sediment surface. This is especially important during periods when the water becomes stagnant and oxygen availability may be limited. Other organisms have similar strategies. Several ciliate species, e.g., *Vorticella* sp., have stalks that allow them to stretch out through the diffusive boundary layer of the substratum to which they are attached.

3.2. Microbial Photosynthesis

3.2.1. Effect of Photosynthesis on Oxygen Microprofiles

As shown in Fig. 9C, microbial photosynthesis can cause high concentrations of oxygen in the photic layers of sediments. The buildup of high oxygen concentrations within the upper layers of a sandy sediment during the first 30 min of a light period is shown in Fig. 12, while the disappearance of the oxygen peak within the first 30 min of the following dark period is shown in the lower portion of the figure. Most of the oxygen peak had actually formed after only 7 min of light incubation, and the steady-state dark profile was approached after only 7 min in the dark.

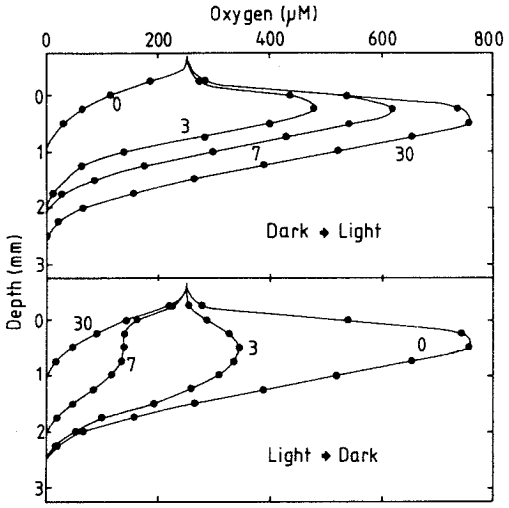

Figure 12. Oxygen profiles in a shallow, sandy sediment from Randers Fjord, Denmark, during a light–dark cycle. The time in minutes after start of illumination at 160 μEinst/m² per sec (dark → light) or darkening (light → dark) is written at each profile. Temperature 22°C.

The sediment analyzed in Fig. 12 had a relatively sparse population of diatoms and was only moderately photosynthetically active. Considerably faster changes and higher oxygen concentrations can be measured in sediments with denser microalgae (Revsbech *et al.*, 1980b), cyanobacterial mats from saline environments (Jørgensen *et al.*, 1979, 1983; Revsbech *et al.*, 1983), or in algal mats from hot springs (Revsbech and Ward, 1983, 1984a,b; Ward *et al.*, 1984).

Changes in oxygen concentration occurring within a sediment during light–dark cycles can be analyzed as in Fig. 12, where each profile was measured by quickly advancing the electrode from the sediment surface and downward, stopping for only a few seconds at 0.25-mm intervals. The disadvantage of this method is that all the data points used to construct the profiles are not measured simultaneously. It took about 1 min to measure a total oxygen profile from top to bottom, and the times written on each profile in Fig. 12 indicate only the start of the measurement. It is also possible, however, to fix the electrode tip at some depth in the substratum and then record the oxygen concentration continuously at that particular depth. A copy of the recorder output from such an experiment is shown in Fig. 13. The sediment was the same as analyzed in Fig. 12, but the light intensity was higher. The electrode was fixed at 0.75 mm depth within the dark-incubated sediment, and the sediment was then illuminated for 16 min. A high steady-state oxygen concentration of 1460 μM O_2 was approached at the end of the light incubation. When the light was turned off, the oxygen concentration decreased rapidly, and after 16

min in the dark, the former steady-state oxygen concentration in the dark was approached.

3.2.2. *Photosynthetic Rates Measured with Microelectrodes*

3.2.2a. Principle of Method. The stable oxygen concentration approached when the sediment had been exposed to light for 16 min (Fig. 13) must be the result of an equilibrium between oxygen-consuming and oxygen-producing processes at each depth. The processes removing oxygen from any particular layer are (1) biological and chemical consumption of oxygen within this layer and (2) molecular diffusion away from the layer. The only process that produces oxygen is oxygenic photosynthesis as carried out by microalgae and cyanobacteria. When photosynthesis was stopped instaneously by darkening (Fig. 13), consumption and diffusional transport of oxygen continued at initially unchanged rates. There was, however, no longer a production of oxygen to counterbalance the losses of oxygen, and the oxygen concentration therefore started to decrease at a rate equal to the former photosynthetic rate. Measurement of the initial rate of decrease in oxygen concentration after darkening can thus be used to quantify the photosynthesis of the oxygenic phototrophs (Revsbech *et al.*, 1981) in systems where these organisms are concentrated, e.g., in shallow water sediments and in epiphytic communities.

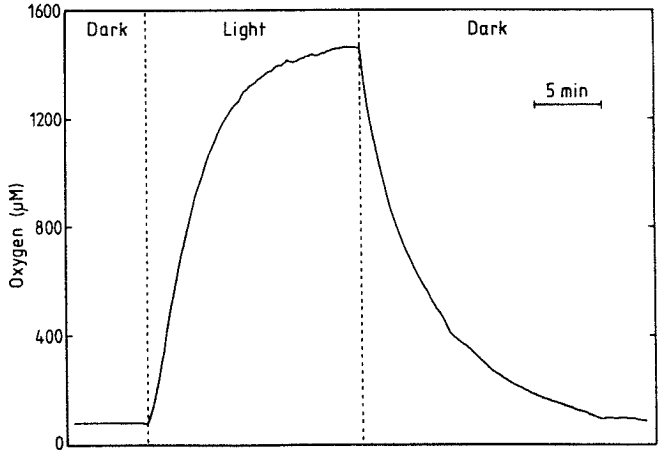

Figure 13. Continuous recording of oxygen concentrations at 0.75mm depth in a sandy sediment during a light–dark cycle. The sediment was taken from 0.5 m water depth in Randers Fjord, Denmark. The light intensity was 700 μEinst/m^2 per sec; temperature, 22°C.

The arguments above can also be expressed mathematically using Fick's second law of diffusion (Crank, 1983). In the light, the change in oxygen concentration $C(x,t)$ at depth x over time t is given by

$$\frac{\delta C(x,t)}{\delta t} = D_s \frac{\delta^2 C(x,t)}{\delta x^2} - R(x,t) + P(x,t) \tag{2}$$

where $R(x,t)$ is the rate of oxygen consumption and $P(x,t)$ is the rate of oxygen production. D_s is the apparent diffusion coefficient of oxygen in the substratum. At steady state in the light, $\delta C(x,t)/\delta t = 0$, and Eq. (2) can be written

$$P(x,t) = -\left[D_s \frac{\delta^2 C(x,t)}{\delta x^2} - R(x,t) \right] \tag{3}$$

In the dark, $P(x,t) = 0$, and Eq. (2) can be written

$$\frac{\delta C(x,t)}{\delta t} = D_s \frac{\delta^2 C(x,t)}{\delta x^2} - R(x,t) \tag{4}$$

Immediately after darkening, the oxygen gradients have not changed significantly, and the value of the diffusion term in Eqs. (3) and (4) is therefore the same. The rate of oxygen consumption $R(x,t)$ in the light and just after turning off the light can also be assumed to be the same [discussed by Revsbech and Jørgensen (1983)]. Therefore, by combining Eqs. (3) and (4) one obtains

$$P(x,t) = -\frac{\delta C(x,t)}{\delta t} \tag{5}$$

Equation (5) expressed that the initial rate of decrease in oxygen concentration after darkening equals the former gross photosynthetic rate.

3.2.2b. Capabilities and Limitations of the Method; Comparison with Other Methods. Comparison of the oxygen microelectrode method wtih conventional methods for measuring photosynthesis showed agreement in some systems (Revsbech *et al.*, 1981). The limitations suggested by our first report on the new method seemed largely to be due to the long, 1-min dark incubations we used, during which the oxygen gradients changed considerably. The rate of decrease in oxygen concentration should preferably be read within a few seconds of darkening while the decrease is still linear with time. The spatial resolution of the method was shown to be 0.1 mm when the rate of decrease in oxygen concentration

was measured over only 1 sec (Revsbech and Jørgensen, 1983). Using the initial rate for calculating the photosynthesis recommended by Revsbech and Jørgensen (1983) should probably be avoided, as some electrodes are slightly sensitive to light (Baumgärtl and Lübbers, 1983). The small change in the reading because of this artifact occurs instantaneously during light–dark changes and is usually insignificant, but it might cause problems during quantification of very low rates of photosynthesis. The possible effect of light on the oxygen microelectrodes can be checked in media without photosynthetic activity, e.g., sterile water. In addition to the direct effect of light on the response of the oxygen microelectrodes, there may also be an effect from heating. The oxygen microelectrodes are highly sensitive to changes in temperature (Baumgärtl and Lübbers, 1983; Revsbech and Ward, 1983), and a temperature drop associated with darkening may result in a decrease in the signal, which could be misinterpreted as photosynthetic activity. Controls with photosynthesis measurements in inactivated sediment should be carried out to check this source of error.

The advantages of the oxygen microelectrode method for measuring microbial photosynthesis in stagnant media are numerous: No other method has similar spatial and temporal resolutions. The result of the measurement is known within seconds, and a new measurement can be taken as soon as a stable oxygen concentration is reestablished, usually within 0.5–1 min. The method is nondestructive, and repetitive measurements can be made on the same cluster of microalgae. Also, methodological errors are under better control than in other methods (Revsbech *et al.*, 1981).

Two other methods have been used extensively to quantify the photosynthetic activity of benthic and epiphytic microalgae. The ^{14}C method is based on the determination of the assimilation of radioactively labeled bicarbonate, whereas the oxygen exchange method is based on the measurement of the oxygen exchange between the substratum and the overlying medium during light–dark cycles. Both methods suffer from inherent methodological problems.

The ^{14}C method (Steemann-Nielsen, 1952) has been used extensively for the quantification of planktonic primary productivity, and the sources of error inherent in the technique have been investigated thoroughly (e.g., Lean and Burnison, 1979). Additional complications arise, however, when the ^{14}C methodology is adapted for use in stagnant media such as microbial films and sediments. It is very important to know the specific radioactivity of the total pool of dissolved inorganic carbon in the environment where photosynthesis takes place, but unfortunately there is no method to assess accurately the specific activity in the microlayers that are photosynthetically active in such substrates. Revsbech *et al.* (1981)

reported that the specific activity of bicarbonate in the photic zone of sediments could be severalfold lower than in the overlying water.

The oxygen exchange method (e.g., Hunding and Hargrave, 1973) is based on the assumption that the photosynthetic rate equals the difference between the oxygen outflux from the sediment in the light and the oxygen influx to the sediment in the dark. It is, however, likely that the increased oxygen availability in the light (see Fig. 9) increases the rate of oxygen consumption in the light compared to the rate in the dark. Stirring gives a much smaller increase in the oxygen availability to the sediment compared to light (Fig. 9), and stirring alone is able to increase the oxygen uptake of sediments very considerably (Pamatmat, 1971; Jørgensen, 1977). The oxygen exchange method will therefore tend to underestimate the actual rate of photosynthesis.

The oxygen microelectrode method, however, also has its limitations. To be sufficiently sensitive, the method requires high photosynthetic rates per unit volume, preferably >2 mmole O_2/dm^3 per hr. It was not possible, for example, to quantify the photosynthesis within lichens, as these rates were too low (M. Sonesson and N. P. Revsbech, unpublished data). Other methods should be chosen when working with substrata having such low activities. Also, the environmental conditions should be reasonably stable during the experiment. For example, fluctuating light intensities caused by drifting clouds during outdoor experiments will make it virtually impossible to obtain stable readings. Mechanical instability of the substratum is another problem often encountered. It is not an advantage to be able to measure photosynthesis with 0.1 mm spatial resolution if the substratum moves 1 cm up or down during the measurement! Macrofauna in the substratum often create problems as the animals cause instability of the oxygen profiles in the surrounding substratum.

3.2.2c. Examples of Microprofiles of Photosynthesis. Profiles of photosynthetic rate have been measured in a variety of sediments and algal mats (Revsbech *et al.*, 1981, 1983; Jørgensen *et al.*, 1983; Revsbech and Jørgensen, 1983; Revsbech and Ward, 1983; 1984b). Examples of photosynthesis and oxygen profiles in a microbial mat in which filamentous cyanobacteria were the dominating phototrophs are shown in Fig. 14. The photosynthetically active layer was only 0.4 mm thick, but a very high maximum rate of 190 mmole O_2/dm^3 per hr was measured within this narrow layer. The photosynthesis integrated over all layers was 37 mmole O_2/m^2 per hr. The highest oxygen concentration, 1152 μM, occurred within the photosynthetically active zone, and it corresponded to 97% saturation with pure oxygen. Supersaturation with pure oxygen (PO_2 up to 1.4 atm) has often been observed in such dense cyanobacterial mats. The very compact cyanobacterial layer at the surface of this micro-

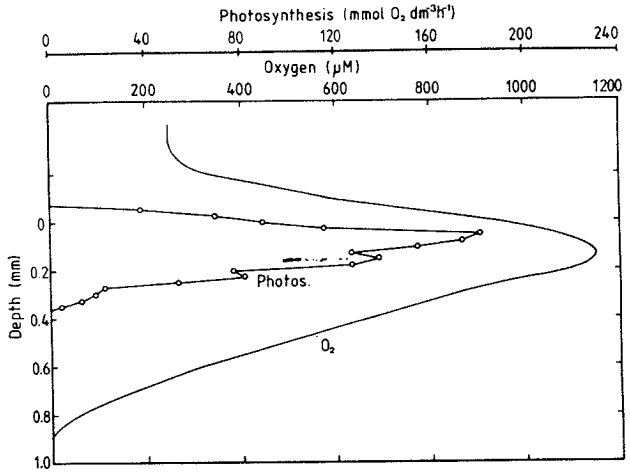

Figure 14. Profiles of oxygen and photosynthesis in an illuminated (250 μEinst/m^2 per sec) cyanobacterial mat from a shallow bay of Limfjorden, Denmark. The cyanobacterial mat was found at the surface of a muddy sediment containing decomposing eelgrass and high sulfide concentrations. Temperature, 21°C.

bial mat caused the light available for oxygenic photosynthesis to be attenuated at 0.4 mm depth. Less dense photosynthetic communities allow a deeper light penetration, for example, diatom communities in coastal sandy sediments where the photic zone may be 2–4 mm thick. An inverse relationship between the rate of photosynthesis per unit volume and the depth of the photosynthetically active layer has been found among microbial mats (Jørgensen *et al.*, 1983; Revsbech and Ward, 1984b).

The high spatial resolution of the photosynthesis determinations by microelectrodes opens possibilities for very detailed analysis of the interactions between environmental factors and the photosynthetic activity in layers or clusters of organisms. The photosynthesis profile can be closely related to the vertical distribution of microorganisms (Jørgensen *et al.*, 1983; Revsbech and Ward, 1984a). In addition, the spatial heterogeneity in the distribution of the photosynthetically active microorganisms can be analyzed in great detail (Revsbech and Jørgensen, 1983).

The effect of incident light intensity on the total photosynthetic rate per unit area, as well as on the vertical distribution of photosynthesis, was analyzed by Revsbech *et al.* (1983) and Revsbech and Ward (1983). These studies indicated that photoinhibition or photosaturation of the investigated microbial mat communities did not occur even at very high light intensities (about 2000 μEinst/m^2 per sec). The surface layers of the

microbial mats were photosaturated, but deeper layers continued to increase in activity with increasing light intensity.

3.2.2d. Computer Modeling of Photosynthetic Rates. As mentioned before, the spatial resolution of the photosynthesis measurement is about 0.1 mm when the rate of decrease in oxygen concentration within 1 sec is used to calculate the photosynthetic rate. A resolution of 0.1 mm may seem adequate for most purposes, but compared to the (e.g., 0.4 mm thickness of the photic layer in dense cyanobacterial mats) 0.1 mm spatial resolution is still rather crude.

The limited spatial resolution of the photosynthesis measurements results in a profile of photosynthesis that is smoothed out when compared to the actual profile. It can be calculated (Revsbech *et al.*, 1986) that the measured rate of photosynthesis at depth x, $P_1(x)$, is related to the actual photosynthetic rate, $P_0(x)$, as follows:

$$P_1(x) = \int_{-\infty}^{+\infty} P_0(y)(4\pi D_s)^{-0.5} \exp\left[-\frac{(x-y)^2}{4D_s}\right] dy \qquad (6)$$

where D_s is the apparent diffusion coefficient for oxygen in the substratum. It is not possible to calculate the actual P_0 values from Eq. (6), but the values can be approximated by computer simulation of a P_0 profile. Experimentally derived rates of photosynthesis are shown in Fig. 15 (solid circles). The straight lines represent an estimated profile of photosynthesis, and the thin curve shows the profile of photosynthesis that would have been measured (P_1) if the estimated (P_0) profile had been the actual profile of photosynthesis. The estimated profile seems to be a good estimate of the actual profile, since the thin curve represents a good fit to

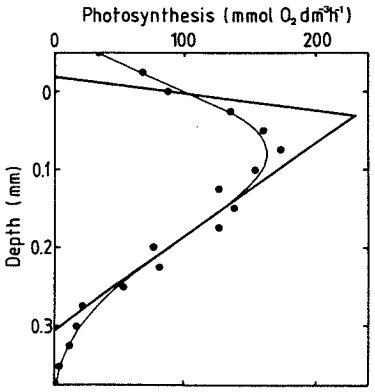

Figure 15. Estimated (P_0) profile of photosynthesis (straight lines) that would have resulted in a measured (P_1) profile of photosynthesis (thin curve) closely simulating the experimentally derived rates of photosynthesis (solid circles, also shown in Fig. 14).

the experimentally derived photosynthetic rates. It is shown in Fig. 15 that the photosynthetic zone as measured by the microelectrodes extends beyond the actual photosynthetic layer. This has also been demonstrated experimentally. It was thus possible to measure photosynthesis in the water above microbial mats (Revsbech and Jørgensen, 1983) if the distance to the photosynthetically active layers was less than 0.1 mm. This reflects why the spatial resolution is only 0.1 mm. Another effect of the limited spatial resolution is that the measured maximum photosynthetic rate is lower than the actual maximum.

3.3. Microbial Respiration

3.3.1. Total Oxygen Uptake

The oxygen uptake of sediments (or biofilms, detritus, etc.), much of which is due to microbial respiration (Dale, 1978), can be calculated from the slope of the linear oxygen concentration profile through the true diffusive boundary layer (Section 3.1.3) above the sediment surface, using the one-dimensional version of Fick's first law of diffusion (Berner, 1980):

$$J = -\phi D_s \, \delta C(x)/\delta x \tag{7}$$

where J is the flux of molecules through a unit area per unit time, D_s is the apparent (Berner, 1980) diffusion coefficient of oxygen in the substratum, ϕ is the porosity ($\phi = 1$ in water), and $C(x)$ is the concentration of molecules at depth x.

As an example, the oxygen gradient just above the sediment surface shown in Fig. 5 indicates an oxygen import to the sediment of 2.6 μmole/cm^2 per day, assuming a diffusion coefficient in the diffusive boundary layer of 2.1 cm^2/sec (Broecker and Peng, 1974). An oxygen uptake rate of 0.2 μmole/cm^2 per day in a deep sea sediment from 3750 m water depth has also been calculated from oxygen microprofiles (Reimers and Smith, 1986). Instead of the oxygen gradient in the diffusive boundary layer above the sediment, these authors used the oxygen gradient immediately below the sediment surface for the flux calculation and therefore needed to estimate the porosity and the apparent diffusion coefficient in the sediment. Their calculated oxygen uptake and the rate of sediment community oxygen consumption determined *in situ* by use of a belljar approach were not significantly different. Similar comparisons between the two methods applied to shallow water sediments usually resulted in the estimates obtained by the flux calculations being 10–50% lower than the figures obtained by belljar methodology (B. B. Jørgensen, unpublished results). This discrepancy is partly caused by the respiration of the abun-

dant infauna inhabiting shallow sediments and by the oxygen consumption of the sediment surfaces within infaunal burrows, but some of the difference may also be due to the irregular surface topography of the sediment surface. In deep sea sediments, the burrowing fauna is much sparser than in shallow sediments, and the additional oxygen consumption caused by infauna seems to be insignificant (Reimers and Smith, 1986).

3.3.2. Depth Profiles of Oxygen Consumption

Unfortunately, a high-resolution method is not readily available for respiration measurements with microelectrodes similar to the one for photosynthesis. It is, however, possible to calculate the oxygen consumption at various depths in a substratum by computer simulation of measured oxygen profiles in light and dark.

The change in the oxygen profile with time is given by an extended version of Fick's second law of diffusion (Berner, 1980):

$$\frac{\delta C(x,t)}{\delta t} = D_s(x)\frac{\delta^2 C(x,t)}{\delta x^2} + \left[\frac{\delta D_s(x)}{\delta x} + \frac{D_s(x)}{\phi(x)}\frac{\delta \phi(x)}{\delta x}\right]\frac{\delta C(x,t)}{\delta x} + P(x,t) - R(x,t) \tag{8}$$

where $C(x,t)$ is again the oxygen concentration at depth x and time t, $D_s(x)$ is the apparent diffusion coefficient, $\phi(x)$ is the porosity, $R(x,t)$ is the oxygen consumption, and $P(x,t)$ is the oxygen production. Equation (8) is an extension of Eq. (2) and can be used to model the oxygen profiles when the diffusion coefficient and the porosity vary with depth. Equation (8) is a one-dimensional model for the oxygen in the sediment, and it will consequently only give a satisfactory description if lateral heterogeneity is small. The oxygen consumption $R(x,t)$ can be calculated from Eq. (8) if the oxygen profiles are sufficiently well described and if the other parameters in the equation are known.

It was shown in Section 3.2.1. how the vertical profile of photosynthesis $P(x,t)$ can be determined. It is, however, also necessary to know the vertical distribution of diffusion coefficients D_s and porosity ϕ to make use of Eq. (8). The porosity can be calculated from the weight loss of a known volume of sediment after drying, but it is difficult to get a sufficiently good depth resolution of ϕ this way. The diffusion coefficient can be determined by measuring the down-diffusion of oxygen into a sterilized, air-exposed, and fully oxidized sediment core subjected to a sudden change in the overlying atmosphere from air to 100% oxygen. The diffusion coefficient can then be read from an inverse error function plot as described by Duursma and Hoede (1967). This method (Revsbech *et al.*,

1986) gives only one estimate of the diffusion coefficient and not a vertical profile, but such vertical profiles can be obtained by scraping off thin layers of surface sediment and consecutively measuring the diffusion of oxygen into these newly exposed surfaces. The depth resolution of the diffusion coefficient can be about 1 mm using this procedure. New computerized methods are now being developed to improve the estimates of diffusion coefficients and porosities in the surface layers of sediment (N. P. Revsbech, unpublished data).

In the simple case of a steady-state oxygen profile [$\delta C(x,t)/\delta t = 0$] and no photosynthetic activity [$P(x,t) = 0$], and when D_s and ϕ are known, it is quite simple to calculate the rate of oxygen consumption at various depths using Eq. (7) or Eq. (8). When the oxygen profile is not in a steady state, it is necessary, however, to perform computer simulation of the oxygen profiles to obtain reasonably accurate estimates of the rates of oxygen consumption in various layers. Very rapid changes in the oxygen profile may occur after changes in the environmental conditions. The development in the oxygen concentration at various depths in a microbial mat after turning off the light is shown in Fig. 16. The steady-state oxygen profile in the light and the measured profile of photosynthesis from this site are shown in Fig. 14. The diffusion coefficient and porosity

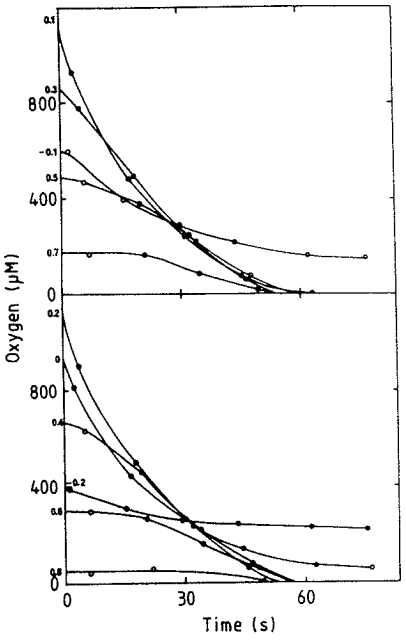

Figure 16. Oxygen concentrations at various depths in the cyanobacterial mat after turning off light. The steady-state starting profile of oxygen during illumination is shown in Fig. 14.

in the uppermost 1 mm layer were found, as described above, to be 1.5 $\times$ 10^{-5} cm^2/sec and 0.95, respectively.

The steady-state oxygen profile shown in Fig. 14 was modeled from Eq. (8) using an iterative computer method [Crank-Nicholson method (Crank, 1983)]. Satisfactory simulations of both the steady-state oxygen profile in the light and the transient oxygen profiles developing after darkening were obtained (Fig. 17) by using the P_0 profile of photosynthesis shown in Fig. 15 and the profile of oxygen consumption shown in Fig. 18. All photosynthesis values shown in Fig. 15, however, had to be multiplied by a factor of 1.248 for the simulation to yield good approximations to both steady-state and transient profiles. This factor varied from 0.79 to 1.248 when five sets of data like those shown in Figs. 14 and 16 were analyzed (Revsbech *et al.*, 1986). The need to multiply by a factor different from 1 is an indication of lateral heterogeneity. As a result of the high spatial resolution of the photosynthesis measurements, only the microbial mat closer than 0.1 mm to the site being analyzed contributes significantly to the measured rate of photosynthesis (Section 3.2.2b). The oxygen concentration profile, however, is influenced by the production rates of oxygen much further away than 0.1 mm. A three-dimensional diffusion model could compensate for this, but it would require an unrealistic amount of experimental data. The multiplication factor mentioned above was introduced to compensate for the inability of a one-dimensional model to include the effect on the oxygen profile of neigh-

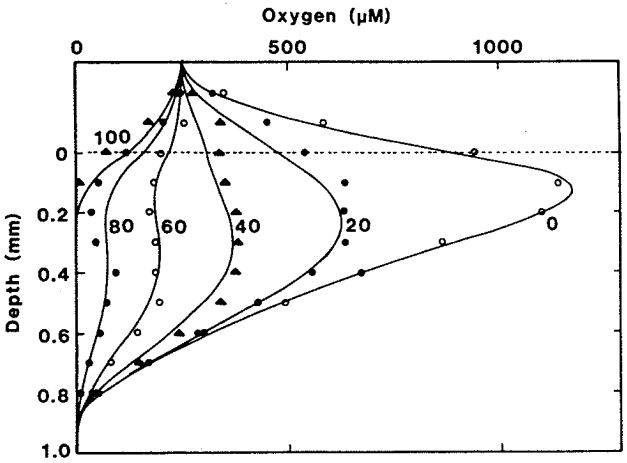

Figure 17. Oxygen profiles after a light–dark shift simulated by use of Eq. (8) and inserting the values of respiration and photosynthesis shown in Figs. 15 and 18. The solid circles show the experimentally derived profiles, which were obtained by interpolation between data points shown in Fig. 16.

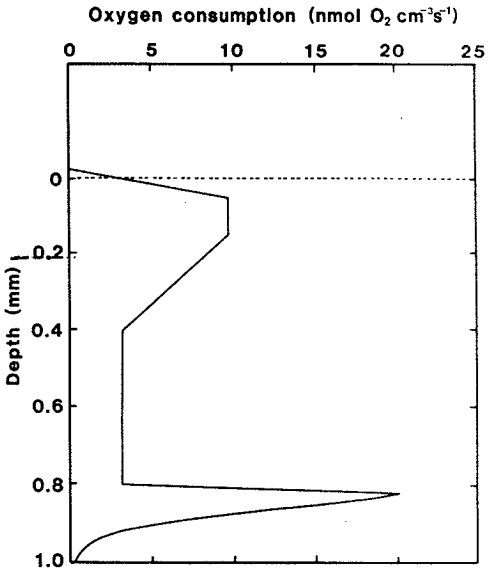

Figure 18. Estimated profile of oxygen consumption that gave a good simulation (Fig. 17) of the oxygen data shown in Figs. 14–16.

boring sites with different net production rates of oxygen. The proximity of the multiplication factors to unity (mean value 1.03) shows that the algal mat was only moderately heterogeneous. This was also suggested by the similarity of the five measured profiles of photosynthesis and oxygen concentration (Revsbech *et al.*, 1986).

Of the five sets of data analyzed, all oxygen consumption profiles showed a maximum of oxygen consumption in the lower part of the photic zone and another maximum at the oxic–anoxic boundary. The upper maximum was probably due to microbial respiration of photosynthates and degradation of senescent microbial cells accumulating in this layer. The lower maximum was associated with the extensive oxidation of reduced inorganic compounds in this layer, especially of sulfide (Revsbech *et al.*, 1983; Jørgensen and Revsbech, 1983).

3.4. Microbial Sulfide Oxidation

Oxygen is a key factor in the environment and exerts great control over all biological processes. In the oxic parts of the world, aerobic respiration is the dominant factor in energy metabolism, and complete oxidative pathways are present within the individual cells. In the anoxic world, bacterial fermentations and anaerobic respiration yield a range of reduced organic or inorganic end products, which are excreted from the cells. The oxic–anoxic interface thereby becomes an important site for the

reoxidation of these reduced compounds. With one notable exception, the sulfide electrode, suitable microelectrodes to detect these compounds still need to be developed.

Microorganisms specially adapted to life at the oxic–anoxic interface are well known. Heterotrophic bacteria often reveal the position of the interface by the formation of narrow bands in stagnant liquid cultures at a certain distance from the medium surface. In liquid enrichment cultures with a heavy inoculum of soil or organic debris, such microaerophilic bacteria can sometimes be observed swarming just over the solid substratum. It has been inferred from independent knowledge of the aerobic metabolism of the bacteria and perhaps also of their low oxygen tolerance that their position here was just at the oxic–anoxic interface. Their adaptation to microoxic conditions can now be demonstrated by direct measurements with an oxygen microelectrode.

Aerobic, heterotrophic bacteria, which through the chemotactic response are able to aggregate in the microoxic zone, may also find in this environment the optimal supply of organic substrates, which diffuse out of the anoxic zone. Many chemoautotrophic bacteria are also highly adapted to this environment, where inorganic compounds such as H_2, NH_4^+, H_2S, and Fe^{2+} serve as electron donors for their energy metabolism. The specialized sulfur and iron bacteria, which are adapted to oxidize H_2S and Fe^{2+}, are in the unusual situation of having to compete with a simultaneous chemical oxidation of their energy substrates by oxygen (Jørgensen, 1982). They are therefore closely tied to the oxic–anoxic interface, where they live between the opposed gradients of their electron donor and acceptor. These fascinating gradient bacteria have been difficult to study because of the insufficient spatial resolution of the analytical techniques. Microelectrodes now provide a powerful tool for studying the ecology of the sulfide-oxidizing bacteria.

3.4.1. Life at the O_2–H_2S Interface

Most sulfide oxidation in nature takes place within sediments at depths of several centimeters from the surface, where it is difficult to discriminate the sulfide oxidizers quantitatively from other bacterial populations (Jørgensen, 1983). In sediments with a high organic turnover, however, high rates of oxygen consumption and sulfate reduction may push the O_2–H_2S interface up to the sediment–water interface. Under these conditions, mass development of colorless sulfur bacteria such as the filamentous *Beggiatoa* spp. can sometimes be observed on the sediment surface. An example of such a *Beggiatoa* mat is shown in Fig. 19 together with the oxygen distribution as measured by microelectrodes (Jørgensen and Revsbech, 1983). The two-dimensional map of isopleths

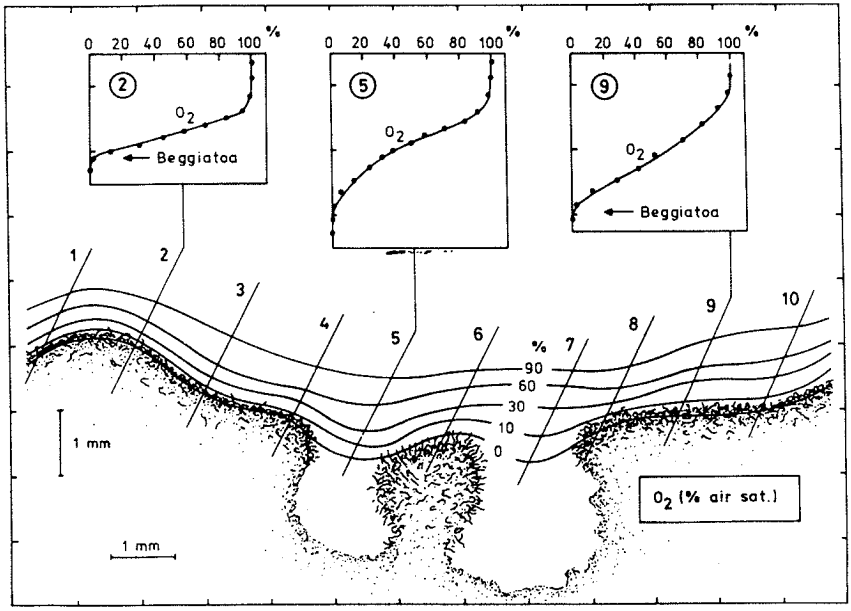

Figure 19. Vertical section through a *Beggiatoa* mat that grew on the sulfide-rich mud in a Danish fjord. Oxic water was flowing over the mud surface. Ten oxygen microprofiles, three of which are shown in insert, were used to construct the O_2 isopleths. Numbers indicate percent air saturation. [From Jørgensen and Revsbech (1983).]

was constructed from an array of vertical O_2 profiles in a similar manner as in Fig. 11.

Although the sediment was covered by circulating, aerated seawater, the bacteria were living under microoxic or anoxic conditions. This is due to the presence of the diffusive boundary layer (Section 3.1.3) and to the high oxygen uptake of the bacteria themselves. The oxygen uptake was limited only by the diffusion flux through the boundary layer, and the potential oxygen uptake of the *Beggiatoa* mat was much higher than the actual uptake. This could be seen either by increasing the water flow and thereby decreasing the thickness of the diffusive boundary layer or by increasing the oxygen concentration in the water. The diffusive flux of oxygen into the bacterial mat simply increased in proportion to the steepness of the oxygen gradient in the boundary layer, while the mat itself remained anoxic.

The combination of an oxygen transport barrier provided by the diffusive boundary layer and the high bacterial metabolism may lead to anoxia in many other environments that one would intuitively expect to be oxic. Thus, the surface of detritus particle and sediments, of biofilms

on rocks and plants, etc., may also be microoxic at the very surface (Jørgensen and Revsbech, 1985). This phenomenon can explain why anaerobic bacteria, such as purple sulfur bacteria in a sulfuretum, can grow on surfaces seemingly exposed to high oxygen concentrations. The oxygen isopleths in Fig. 19 show how the diffusive boundary layer covered the bacterial mat like a 0.5- to 1-mm-thick blanket of water that followed the coarser surface topography.

The position of the O_2–H_2S interface within the *Beggiatoa* mat is shown in detail in Fig. 20. The mat was again covered by flowing, aerated seawater with a uniform oxygen distribution. A sharp drop in oxygen concentration was observed within the 0.5-mm-thick diffusive boundary layer of the mat. On the expanded scale (Fig. 20, right) the oxygen is seen to penetrate only 100 μm into the mat. A steep H_2S gradient started from 50 μm below the mat surface and the H_2S level increased to 500–1000 μM a few centimeters deeper in the black mud. The zone in which both oxygen and sulfide coexisted in the mat was thus only 50 μm thick. Within this narrow layer, all sulfide produced in the sediment and diffused to the surface evidently became oxidized. The zone extended only over one-tenth of the total thickness of the 0.5-mm *Beggiatoa* mat, which

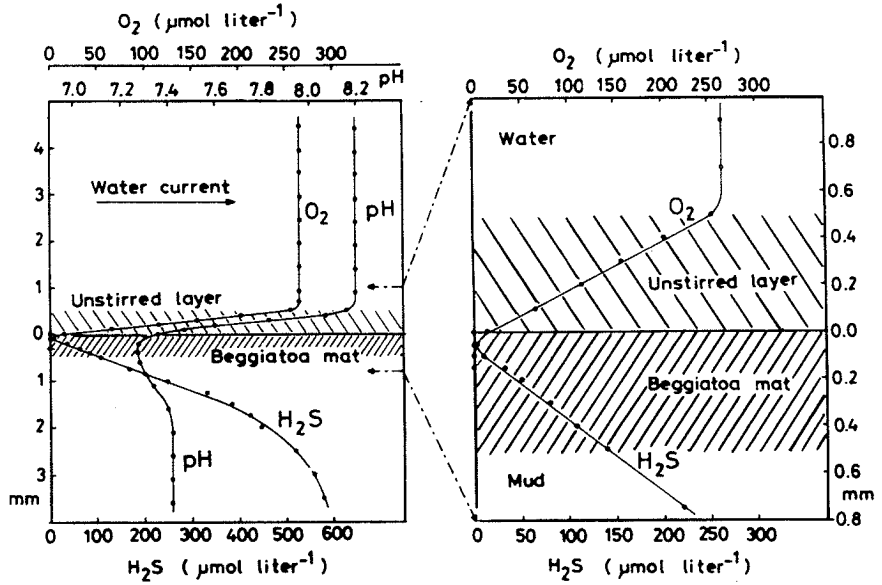

Figure 20. Oxygen, sulfide, and pH microgradients through a *Beggiatoa* mat that grew on a mud surface under flowing, aerated seawater. The expanded depth scale shows the 0.5-mm-thick mat with the narrow O_2–H_2S interface and the overlying diffusive boundary layer. [From Jørgensen and Revsbech (1983).]

meant that only a small fraction of the bacteria had access to both substrates at any given time.

At the time when the measurements described above were first done, chemoautotrophic growth of *Beggiatoa* in pure cultures with H_2S as the sole energy source had not yet been proven. Calculations of the high H_2S turnover rate in the *Beggiatoa* mat in Fig. 20 showed, however, that this process had to be biological rather than chemical. The first unequivocal demonstration of chemoautotrophy in a marine *Beggiatoa* strain was achieved shortly after by Nelson and Jannasch (1983). They also observed this chemoautotrophic metabolism when the organisms were grown in gel-stabilized gradients of O_2 and H_2S. Recent microelectrode studies of such gradient-grown *Beggiatoa* cultures have confirmed the results obtained from the natural mats and have also demonstrated the potential uses of microelectrode techniques for the study of gradient bacteria in general (D. C. Nelson, N. P. Revsbech, and B. B. Jørgensen, in preparation).

One important piece of information that can be derived from such microelectrode data is the overall stoichiometry of the bacterial metabolism. This can be done from simple flux calculations as described in Section 3.3.1. As the calculation of a flux involves the product of the gradient and the molecular diffusion coeffcient of the chemical species, the diffusion coefficient needs to be determined experimentally in the growth medium. This can be done either with microelectrodes or with chemical or radiotracer techniques by tracing the propagation through the medium of an increase or decrease, in concentration (see Section 3.3.2). Other information that can be obtained concerns the interactions between the opposed chemical gradients and the gradient bacteria, the overlap and turnover of the chemical species as a function of the bacterial growth, and even the growth yield of the bacteria.

As an example, results from the gradient culture system described by Nelson and Jannasch (1983) are shown in Fig. 21. The O_2, H_2S, and pH profiles were measured through two test tubes with seawater partly solidifed with agar. The lower 2 cm of the agar initially contained 4 mM H_2S, while the upper agar layer was free of H_2S and only contained mineral salts. One of the tubes was inoculated with a chemoautotrophic strain of marine *Beggiatoa.* The situation after 3–4 days when the H_2S had diffused up to reach the lower boundary of the oxic surface layer is shown in Fig. 21. In the uninoculated tube, O_2 and H_2S overlapped by 5–6 mm and there was only a small pH effect derived from the relatively slow, chemical sulfide oxidation. In the inoculated tube, *Beggiatoa* grew in a 0.4-mm-thick horizontal band just at the sharp O_2–H_2S interface. Coexistence of the two substrates could only be measured in a 50-μm-thick zone, which demonstrated a very efficient uptake and oxidation of H_2S

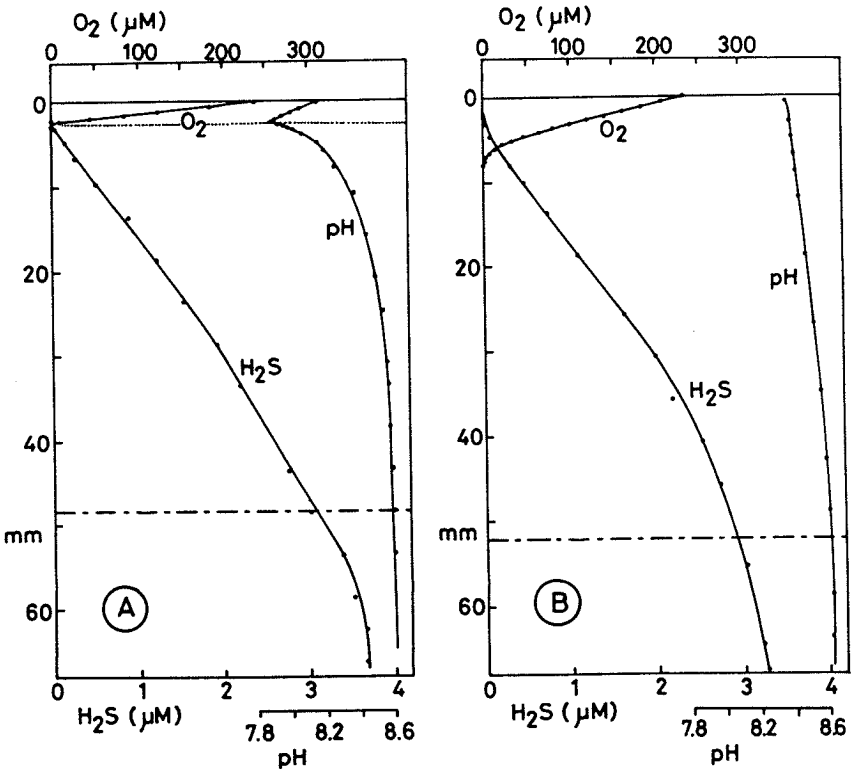

Figure 21. Gradient culture of a marine *Beggiatoa* (strain MS-81-6). (A) The oxygen, sulfide, and pH gradients 3 days after inoculation, showing the sharp O_2–H_2S interface within the *Beggiatoa* mat (dotted line). (B) Uninoculated control after 4 days, showing a broad O_2–H_2S overlap. [Data from D. C. Nelson, N. P. Revsbech, and B. B. Jørgensen (in preparation).]

by the bacteria. The mean residence time of O_2 and H_2S in the overlap zone was only a few seconds. The oxidation of H_2S to sulfuric acid caused a sharp minimum in pH. An oxidation to sulfuric acid was in agreement with the calculated ratio between H_2S and O_2 fluxes.

Throughout the rapid growth phase, which was linear due to constant diffusion limitation, the ratio of H_2S/O_2 consumption in the *Beggiatoa* mat was about 0.6. If all H_2S was oxidized to sulfuric acid, the ratio would be 0.5. The slightly lower oxygen consumption was found not to be due to a lower oxidation state of the sulfur product, i.e., due to the formation of elemental sulfur, which was only a transient oxidation product, but to the reduction of CO_2. Thus, about 15% of the electrons from H_2S were transferred to CO_2 and the rest to O_2. In accordance with this

finding, the increase in bacterial biomass corresponded to a growth yield of 8 μg/μmole H_2S. This is slightly higher than for aerobic thiobacilli (Kelly, 1982) and shows that *Beggiatoa* cells are well adapted to a chemoautotrophic mode of life at the O_2–H_2S interface.

3.4.2. H_2S and Photosynthesis

The distribution of oxygen in nature, and thus the position of the O_2–H_2S interface, is highly dependent on light and photosynthetic activity. In shallow waters, benthic microalgae on sediments, rocks, plants, and other solid surfaces produce local oxygen maxima, which push the oxic zone deeper into the substratum as discussed earlier. The diurnal light–dark variations thus create a cyclic pulse of oxygen to which both the photosynthetic organisms and the gradient bacteria need to adapt. In those organic-rich sediments where light penetrates down into the sulfide zone, a similar daily pulse in sulfide concentration may be found due to the activity of photosynthetic sulfur bacteria. As an example of a benthic microalgal community with both high photosynthetic activity and high sulfide concentration, we have studied cyanobacterial mats from the hypersaline Solar Lake in Sinai (Jørgensen *et al.*, 1983; Revsbech *et al.*, 1983). These mats consist mostly of filamentous cyanobacteria, e.g., *Microcoleus* and *Phormidium,* but also contain a variety of coccoid cyanobacteria, heterotrophic bacteria, and colorless and photosynthetic sulfur bacteria. We analyzed the dynamic distributions of O_2, H_2S, and pH in these mats during abrupt light–dark shifts as well as during the natural light variations over a 24-hr cycle. In order to obtain precise depth and time correlations between the three parameters during the light–dark shifts, the three microelectrodes were glued together into one unit with the sensing tips less than 1 mm apart.

Two examples of such simultaneous O_2, H_2S, and pH profiles, one in the dark and one in the light are shown in Fig. 22. The O_2–H_2S interface was situated just 0.5 mm below the mat surface in the dark. The pH decreased steeply from the water value of 8.2 to a mat value of 7.3. Due to the intensive photosynthesis in the light, a sharp maximum of oxygen built up and pushed the O_2–H_2S interface down to a depth of 2 mm in the mat. Concurrently, pH built up due to the photosynthetic CO_2 assimilation to a maximum of 9.3 just below the surface and then dropped by two units over the following 2 mm.

The microgradients in the mat show how dynamic and variable a microbial environment can be. Organisms living at 0.5 mm depth in the mat were exposed to variations from anoxia to over 1 atm partial pressure of oxygen, depending on the light conditions. The corresponding variations at 1.5 mm depth were from 250 μM H_2S in the dark to 500 μM

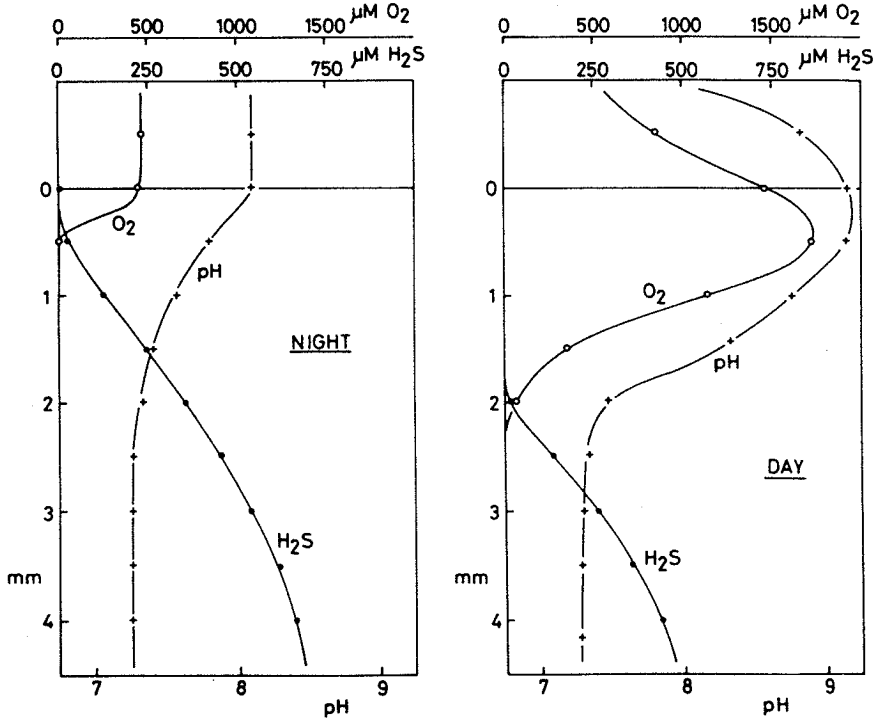

Figure 22. Distribution of O_2, H_2S, and pH in a *Microcoleus* mat from Solar Lake, Sinai, during the night and during the day. [Data from Revsbech *et al.* (1983).]

O_2 in the light. Gradient bacteria associated with the O_2–H_2S interface experienced a vertical movement of their proper chemical environment over 1.5 mm as a result of the light–dark changes. It is probably because of these moving chemical gradients and changing light intensities that most of the dominant mat organisms are motile and can adjust to the changing conditions by migrating up and down. Others, however, remain fixed in the mat structure and may only experience optimal conditions during a limited part of the daily light–dark cycle.

The strong variations in the chemical environment of the mat organisms may seem extreme, but they are not unusual for benthic, photosynthetic communities. Only after the introduction of microelectrodes have such seemingly harsh microenvironments been demonstrated, although they could in fact have been predicted from crude estimates of metabolic rates and molecular diffusion parameters. If the appropriate microelectrodes were available, similar fluctuations could probably also be demonstrated for many other chemical species, such as

NO_3^-, NH_4^+, HPO_4^{2-}, Fe^{2+}, Mn^{2+}, etc., as well as for organic compounds.

A technique to measure anoxygenic photosynthesis by purple or green sulfur bacteria or by cyanobacteria could theoretically be developed based on the initial disappearance rate of H_2S in the light after steady state in the dark. Our experiments with such a technique in microbenthic communities have not been very promising. One serious problem of the technique is the tendency of H_2S to react with elemental sulfur in such systems. This leads to the formation of polysulfides, which rapidly equilibrate with a changing H_2S pool. Relative rates may, however, still give important information on the type and distribution of H_2S-dependent photosynthesis.

One example of such anoxygenic photosynthesis is shown in Fig. 23. The rate of sulfide disappearance after a shift from steady state in the dark to light was followed at 1 mm depth within the same microbial mat (B. B. Jørgensen, Y. Cohen, and N. P. Revsbech, unpublished data). For the present experiment, however, the mat was covered by H_2S-enriched water. The phototrophic mat community depleted the sulfide pool within 5 min and already after 3 min an O_2 pool started to build up. In order to demonstrate whether the sulfide disappearance was due to an anoxygenic photosynthesis or to a secondary oxidation by O_2 of an initially nonde-

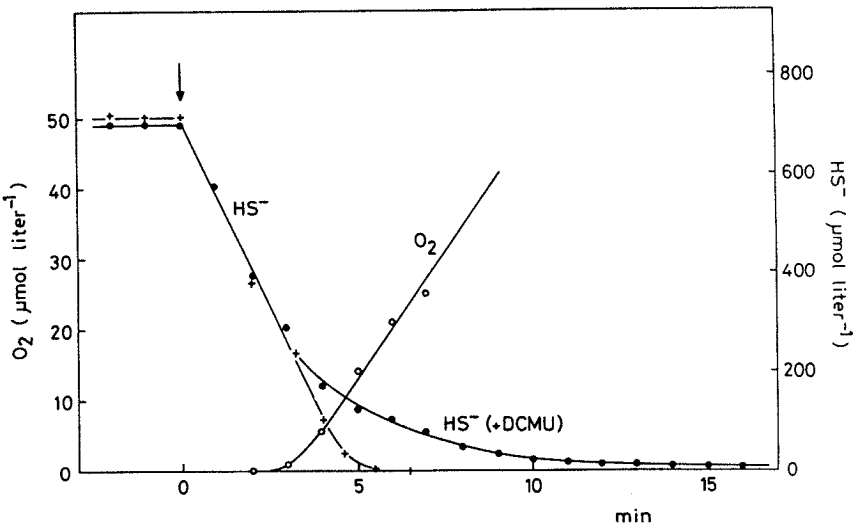

Figure 23. Photosynthetic sulfide oxidation and oxygen production at 1 mm depth in a *Microcoleus* mat after a dark–light shift (arrow). Experiments done without and with DCMU added. [Data from Jørgensen *et al.* (1986).]

tectable concentration, the oxygenic photosynthesis was inhibited by the addition of DCMU [3-(3,4-dichlorophenyl)-1,1-dimethyl-urea]. The initial sulfide disappearence was unaffected by DCMU, which indicated that the phototrophic organisms carried out anoxygenic photosynthesis with H_2S (cf. Cohen *et al.*, 1975a,b). When the sulfide level had dropped below 200 μM, the anoxygenic photosynthesis became inefficient. This was the level at which free O_2 had started to develop in the uninhibited mat. The results of this and other experiments led to the conclusion that oxygenic and anoxygenic photosynthesis may operate in concert in these microbial mats at levels that mostly depend on the sulfide concentration (Cohen, 1984).

By experiments such as the one shown in Fig. 23, the microelectrode techniques allow physiological studies of microbial communities *in situ* without causing physical disturbance to the system.

3.5. Symbiosis

There are many fascinating examples of symbiotic associations between microorganisms and animals. The mutual benefits of the association for the host and symbionts vary, but one classical and widespread example is the symbiosis between microalgae and aquatic invertebrates. This type of association has reached its highest development in tropical, marine environments, where, for example, the growth of coral reefs is dependent on the photosynthetic activity of algal cells imbedded in the tissue of each polyp. Many other examples are known of similar symbiotic associations between microalgae, or just their chloroplasts, the protozoa, sponges, nudibranchs, bivalves, tunicates, etc. (Stanier *et al.*, 1977).

Through the close symbiotic association, an efficient nutrient cycling between algae and the animal host may be achieved, which is especially important in nutrient-poor tropical waters. The algal photosynthesis provides organic carbon, and thus energy, for the host, whereas the host efficiently retains inorganic nutrients, which are recycled to the algae. In addition, the photosynthetic activity may be of significance for the calcification process in hosts that build a calcareous skeleton (Drew, 1973).

Due to the intimate association between autotrophic and heterotrophic processes in algal–animal symbiosis, it is experimentally difficult to analyze the metabolic activity of the two components separately. These problems are in many respects similar to those encountered when other, nonsymbiotic communities are studied. Oxygen and ^{14}C techniques have been used to distinguish respiration and photosynthesis in corals, sponges, foraminifera, etc. Both approaches have serious limitations, however, in the quantitative and spatial separation of the two processes.

Over the last 2 years, we have experimented with the use of microelectrodes to study symbiotic photosynthesis in subtropical waters. With the oxygen microelectrodes it is possible to analyze the oxygen dynamics in the immediate surroundings of the host animal or even to penetrate into the tissue of the host. By rapid light–dark shifts, we could thereby detect and map the gross rate of photosynthesis of the symbionts, independent of the surrounding respiratory activity of the host, by the technique described in Section 3.2.

One example of the oxygen dynamics in a polyp of a common reef-building coral, *Acropora* sp., from the Red Sea is shown in Fig. 24. The freshly collected coral branch was kept in an aquarium with running, aerated seawater at 24°C and was exposed to alternating darkness and light corresponding to full daylight intensity *in situ*. An oxygen microelectrode was positioned in the polyp tissue, about 1 mm below the tentacles, within the narrow ring of symbiotic zooxanthellae. This could be done with little damage to the tissue and without causing contraction of the polyp. The light–dark variation in oxygen tension was rapid and dramatic, especially considering that this was within the body of a living animal. In normal daylight, the oxygen tension rose to 80% of the ambient air saturation, 205 μM. In the dark, the animal tissue became nearly anoxic. Oxygen was also measured in other polyps on the same coral branch. Oxygen concentrations of up to 450 μM were measured in the light, and a few measurements showed anoxic conditions in the dark.

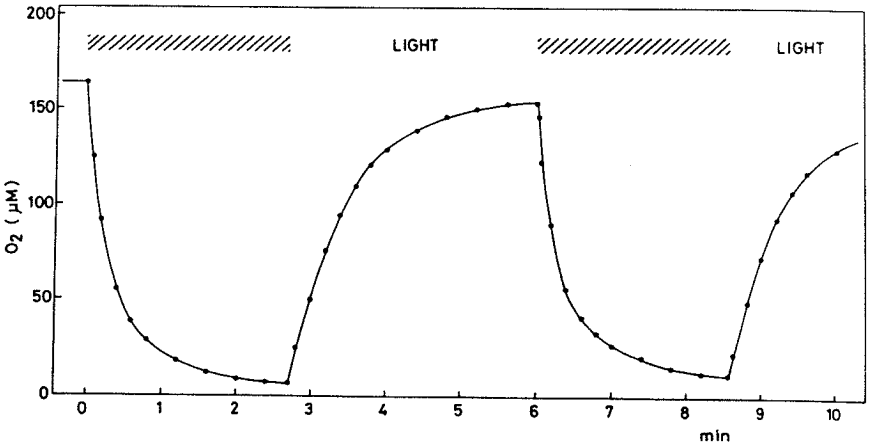

Figure 24. Oxygen concentration in the symbiont-containing polyp tissue of the coral *Acropora* sp. Shifts between darkness and *in situ* daylight (900 μEinst/m^2 per sec) caused rapid variations of PO_2 within the animal. [From N. P. Revsbech, B. B. Jørgensen, and Y. Cohen (in preparation).]

From the initial decrease in oxygen after a light–dark shift (Fig. 24), a photosynthetic rate of 410 μM/min could be calculated. Measurements in other polyps showed photosynthesis rates of up to 3300 μM/min. Due to the complex anatomy of corals and the annular positioning of their symbiont population, it is difficult to calculate the quantitative importance of this symbiotic photosynthesis for the energy metabolism of the whole coral.

Planktonic foraminifera, however, with their small size and spherical symmetry, seem to be ideal systems for such a quantitative analysis. Spinose, symbiont-bearing foraminifera are common in the plankton of tropical oceans (Be and Tolderlund, 1971). These 0.1- to 1-mm protozoa build multichambered shells, which house the protoplast with its multitude of intracellular zooxanthellae (Anderson and Be, 1976). The symbionts are actively spread out by the host around the shell during the daytime. They are imbedded in pseudopodia, which glide out along the radial spines. By carefully approaching the animal between the spines with an oxygen or pH microelectrode it was possible to study the chemical microenvironment of the organisms as well as their metabolic activity. An impression of this microenvironment is given in Fig. 25.

The dimensions of the foraminifer *Globigerinoides sacculifer* with its surrounding halo of intracellular symbionts are shown in Fig. 25A. As the oxygen microelectrode radially approached the shell in the light, the oxygen concentration was found to increase steeply to 2.5 times the ambient air saturation of seawater (Fig. 25B). Thus, the total symbiotic system had a high net photosynthesis. The corresponding decrease of oxygen in the dark reflected the combined respiratory activity of host and symbionts. Rapid light–dark shifts showed that the oxygen pool in the microenvironment was even more dynamic than shown for the coral (Fig. 25C). With a photosynthesis rate of 2700 μM/min at the shell surface, as calculated from the initial oxygen decrease in the dark, the mean residence time of oxygen in the light was only 12 sec. This shows that the oxygen environment of the animal changes sufficiently rapidly to follow closely fluctuations in light intensity due, for example, to clouds passing the sun. In addition, the pH of the seawater around the foraminifer changed according to the intensive CO_2 uptake or release in the light or in the dark, respectively (Fig. 25D).

With the oxygen microelectrode it was possible to map the radial distribution of photosynthesis around the shell as well as to penetrate carefully into the shell (Fig. 26). The measurements were taken at 50-μm increments, each measurement being representative of a 50-μm-thick spherical shell concentrically surrounding the host. Connected values of photosynthesis and spherical shell volumes were then multiplied and summed to yield the total gross photosynthesis of the symbiotic system,

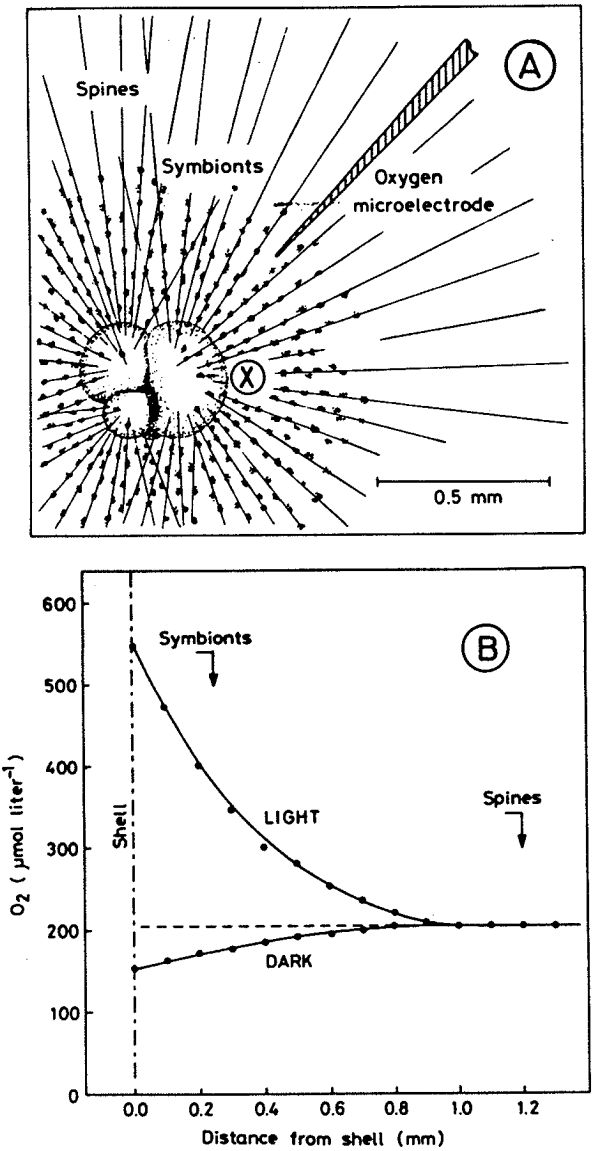

Figure 25. (A) The planktonic foraminifer *Globigerinoides sacculifer*, with its symbiotic zooxanthellae spread out between the spines. The animal was kept in a small glass vessel with water of the Red Sea, where it was collected. (B) Radial gradients of oxygen from the ambient seawater to the shell surface in the dark and in the light. (*continued*)

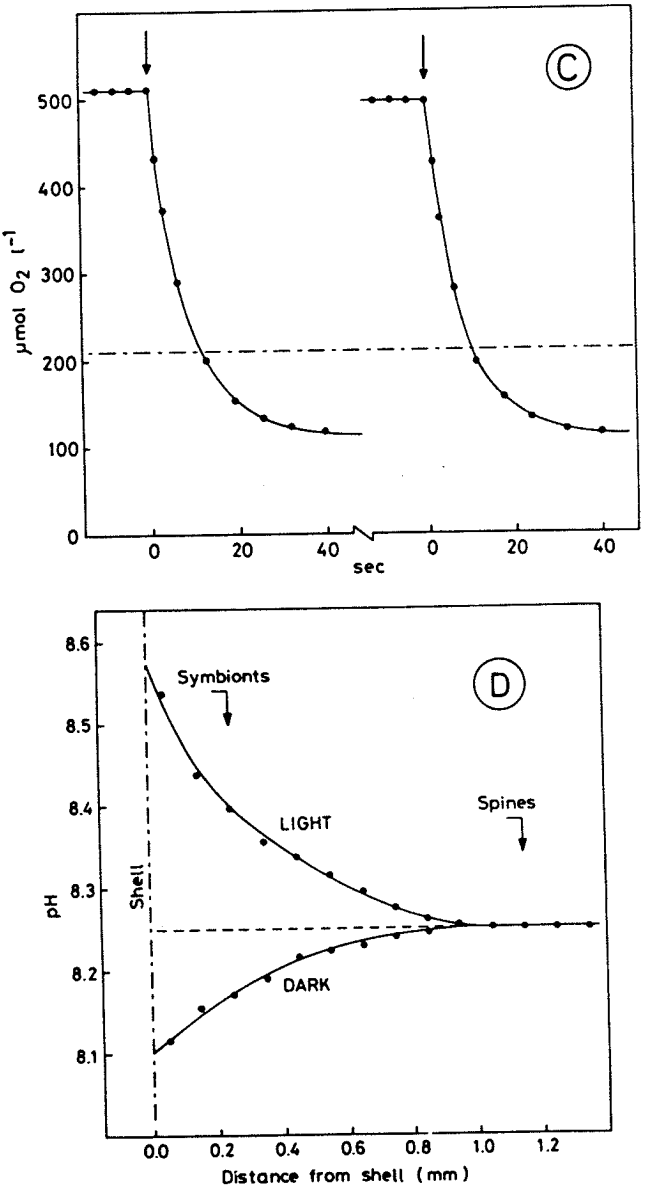

Figure 25 (*continued*). (C) Two experiments showing the rapid decrease in oxygen concentration after a light–dark shift. The electrode tip was positioned at point X shown in A. (D) Radial gradients of pH from the ambient seawater to the shell surface in the dark and in the light. Light intensity was 400 μEinst/m^2 per sec in all experiments; temperature was 24°C. [From Jørgensen *et al.* (1985) and B. B. Jørgensen, J. Erez, and N. P. Revsbech (in preparation).]

18.1 nmole O_2/hr. The net photosynthesis could be calculated from the radial diffusion flux of oxygen over a theoretical sphere of 0.6-mm radius enclosing both host and symbionts. With the O_2 gradient given by dC/dr = 410 μM/mm = 0.41 nmole/mm, the area of the enclosing sphere for r = 0.6 mm of $A = 4\pi r^2$ = 4.5 mm^2, and a diffusion coefficient D = 2.35 $\times$ 10^{-5} cm^2/sec = 8.46 mm^2/hr (Broecker and Peng, 1974), one obtains for the net outward diffusion flux of oxygen from the foraminiferan $J = D(dC/dr)A$ = 15.6 nmole O_2/hr, which is close to the gross photosynthesis of 18.1 nmole/hr. This shows that the symbiotic association is highly autotrophic in the light, and that the symbiont productivity could potentially contribute to the nutrition of the host. Flux calculations of O_2 uptake in the dark based on radial gradients also show a comparatively small dark respiration of 2.7 nmole O_2/hr.

This example shows one great advantage of microelectrode techniques. Due to the small dimensions relevant for microbial environments, the important transport process for gases, ions and other dissolved molecules is predominantly molecular diffusion (Vogel, 1981; Boudreau and Guinasso, 1982; Jørgensen and Revsbech, 1985). A simple mapping of the concentration field around microbial communities may therefore

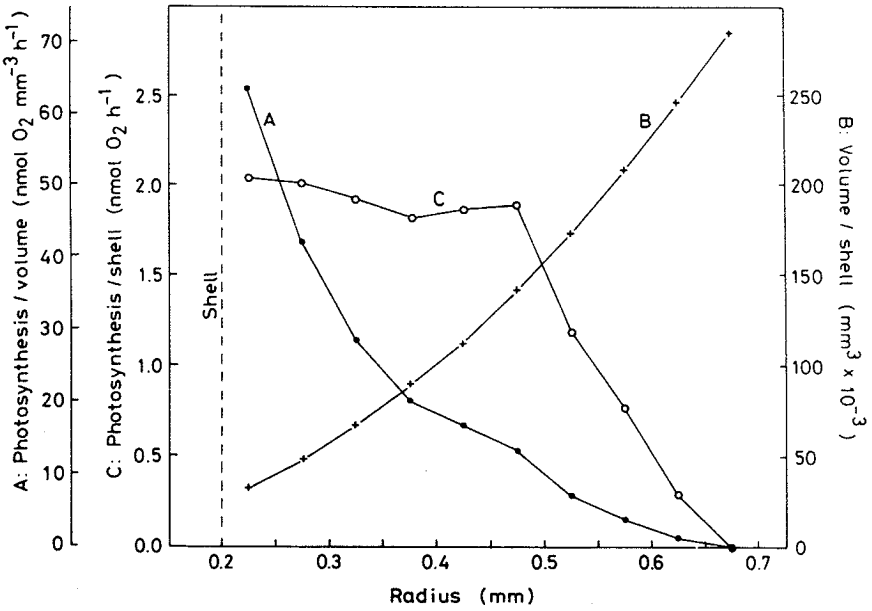

Figure 26. Radial distribution in *G. sacculifer* of (A) rates of photosynthesis per unit volume at 400 μ Einst/m^2 per sec, (B) volume of 50-μm-thick spherical shells, and (C) rates of photosynthesis per spherical shell. [From Jørgensen *et al.* (1985).]

allow the quantitative calculation of their metabolic rates. The planktonic foraminifera provide ideal systems for such studies because of their simple radial symmetry. The laterally uniform, one-dimensional gradients in the sediment systems discussed previously are another example.

Due to the high spatial and temporal resolution of the microelectrode techniques they are also ideally suited for *in situ* studies of the physiology of undisturbed microbial communities. Such an experimental application to the ecological physiology of microorganisms has only just started. In the example of the symbiont-bearing foraminifera, a step in this direction has been the study of photosynthetic adaptation to the ambient light intensity and quality (Jørgensen *et al.*, 1985). These studies were done by keeping the oxygen microelectrode at a fixed position near the shell surface and analyzing the photosynthetic response in relation to the quantum flux and the wavelength of incident light.

The gradual saturation of light-harvesting pigments in the zooxanthellae is shown in Fig. 27. At up to 100 μEinst/m^2 per sec of full-spectrum light, the light reaction in the symbionts limited the photosynthetic rates. Theoretical light saturation I_k was reached at 160 μEinst/m^2 per sec (cf. Harris, 1978). The maximum *in situ* light intensity was reduced to that level only at the 27-m depth in the Red Sea where the animals were collected (Jørgensen *et al.*, 1985). Measurements of radial oxygen micro-

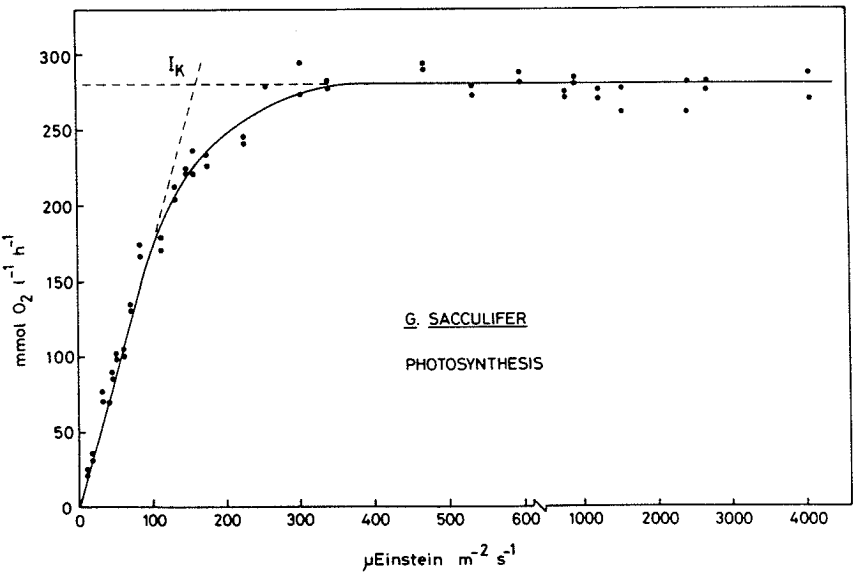

Figure 27. Rate of photosynthesis at the shell surface of a *G. sacculifer* at different light intensities. [From Jørgensen *et al.* (1985).]

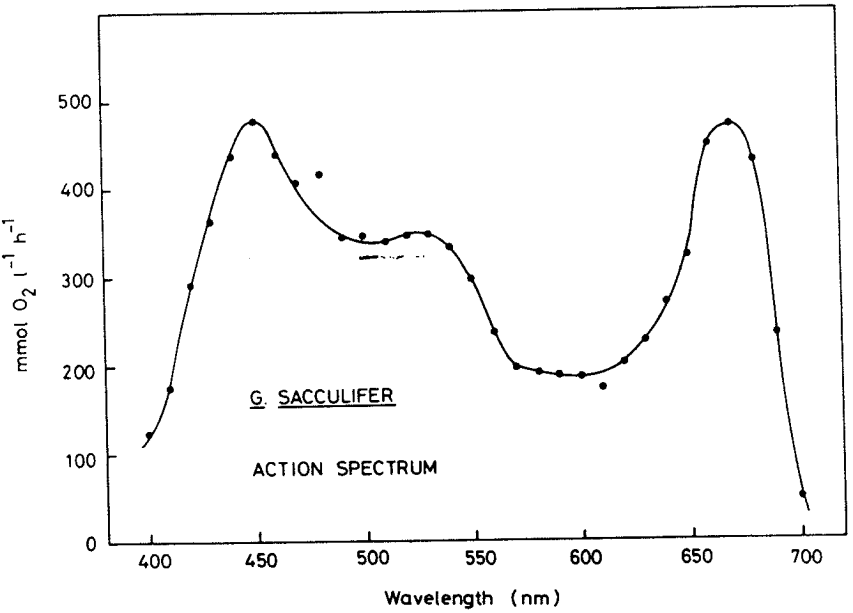

Figure 28. Action spectrum of endosymbiotic zooxanthellae measured at the shell surface of *G. sacculifer*. Photosynthesis maxima show the activity of chlorophyll a and of peridinin. [From Jørgensen *et al.* (1985).]

gradients around the foraminifer at a range of light intensities showed that the compensation light intensity, i.e., the intensity where the gradient was zero due to respiration–photosynthesis balance, was only 30 μEinst/m^2 per sec. This light intensity was reached at 60 m water depth in the Red Sea during midday.

Measurements of photosynthetic rates in monochromatic light at different wavelengths allowed a detailed study of the spectral response of the zooxanthellae. An action spectrum measured at intervals of 10 nm from 400 to 700 nm at a constant quantum flux of 100 μEinst/m^2 per sec. is shown in Fig. 28. Maxima of photosynthetic activity were found at 450 and 670 nm, corresponding to the *in vivo* absorption maxima of chlorophyll a. A broad maximum was also found between 500 and 550 nm. This was due to a protein-bound carotenoid, peridinin, which is an important light-harvesting pigment in dinoflagellates, to which the symbionts belong (Prezelin, 1976; Prezelin *et al.*, 1976; Anderson and Be, 1976). The light absorption by peridinin must be important in the deeper photic zone of the open ocean, where yellow-green light of 500–550 nm is predominant (Jerlov, 1976).

The speed and thus the high analytical capacity of the microelectrode

technqiue are important for measurements such as those in Figs. 27 and 28. The collection of detailed data for the determination of light saturation or action spectra, as presented here, would be much more time-consuming by conventional oxygen or ^{14}C techniques. The data sets shown in Figs. 27 and 28 were each obtained over a few hours. Within such a short period, changes in the photocenters and in pigment composition of the microalgae will be minimal. For this reason, microelectrodes may have a wider and more general application in photosynthesis research in the future.

3.6. Miscellaneous Microenvironments

The microenvironments discussed so far were mostly sediments or symbiotic associations of animals and microalgae. Microelectrodes can also give valuable information about the chemistry and metabolic rates in many other microbial systems. Only a few other microenvironments have been analyzed, but the applications will no doubt increase rapidly over the coming few years. Some examples of potential applications are given below to illustrate the types of information that can be gained from work with microelectrodes.

3.6.1. Soils

The oxygen conditions of agricultural soils are important for the turnover of inorganic nutrients and for the yield of crops. Several attempts have been made to determine the oxygen distribution in soils, using simple oxygen macroelectrodes (e.g., Lemon and Erickson, 1952), membrane-covered macroelectrodes (e.g., Fluhler *et al.*, 1976), minielectrodes (Greenwood and Goodman, 1967), and microelectrodes (Sexstone *et al.*, 1985). The measurements performed by the use of macroelectrodes suffered from poor spatial resolution, and information about the conditions within soil aggregates, which is of utmost importance for the understanding of microbial processes in soil, could not be obtained. The measurements of Greenwood and Goodman (1967), who used an electrode with a tip diameter of 0.5 mm (Naylor and Evans, 1960), were able to show an anaerobic center in artificial, 10-mm soil aggregates. They concluded, however, that their electrode was still too large and might have caused significant disturbance of the conditions within the soil crumb.

Sexstone *et al.*, (1985) used microelectrodes with a tip diameter of 50 μm (Revsbech and Ward, 1983) to measure oxygen gradients in natural, water-saturated soil aggregates. They showed that in this specific soil (Muscatine silty clay loam from Iowa), anaerobiosis often occurred within soil aggregates larger than 6 mm diameter. They also found that

no denitrification occurred within soil crumbs that were oxic in all parts, whereas it did occur in most partly anoxic crumbs. Microelectrode measurements were also used to determine diffusion coefficients for oxygen within the soil crumbs as described in Section 3.3.2.

The measurements of Sexstone *et al.* (1985) were performed in soil crumbs moistened to field capacity. Considerable difficulties would be associated with measurements in soils held at lower water potentials, as the insertion of the electrode in such semidry soil crumbs might cause introduction of air along the electrode shaft. The electrode would also have to be very sturdy to survive an introduction into the semidry crumbs of most soils.

3.6.2. The Rhizosphere

The rhizosphere around roots in soils and sediments is a microenvironment that highly stimulates microbial activity (Alexander, 1977). There is an uptake by the root of inorganic nutrients from the subtratum, and the root may excrete organic substances and oxygen (e.g., Sand-Jensen *et al.*, 1982). The excretion of oxygen by roots can create an oxic microenvironment with an abundance of aerobic bacteria within an otherwise anoxic soil (Joshi and Hollis, 1977). It is important to understand the factors that regulate the distribution of oxygen around roots and how this affects the redox processes in the surrounding soils or sediments. The *in situ* excretion of oxygen from roots has been quantified by "oxygen availability" (Lemon and Erickson, 1952) measurements using polarized rings of platinum surrounding individual roots (Armstrong, 1967). This method, however, is not very satisfactory in several respects. An accurate calibration of the reading to actual oxygen excretion rates is difficult. The method gives a figure only for the excretion and no information about the extension of the oxic zone. Finally, it it is difficult to place the platinum ring without disturbing the root and its environmental conditions to a significant extent.

The oxygen regime around roots can in theory also be measured *in situ* by use of microelectrodes. The problem is to identify the position of the electrode relative to the roots and to advance the microelectrode to a sufficiently great depth without damaging it. Instead of soil, a preliminary study of oxygen gradients around roots was conducted in agar in which the freshwater macrophyte *Littorella uniflora* was growing (P. B. Christensen, N. P. Revsbech, and J. Sørensen, unpublished data). An oxygen microelectrode, similar to the one shown in Figs. 1B and 2, but with a 10-cm-long tip region of less than 2 mm diameter, was used for the experiments. The data obtained showed that it is possible to measure oxygen gradients accurately deep below the water–substratum interface. The

measured oxygen gradients were used to calculate the excretion of oxygen as a function of environmental conditions, such as incident light intensity on the leaves. It was found that the oxygen excretion increased linearly with increasing light intensity up to 70 μEinst/m^2 per sec, where light saturation of the excretion rate (photosynthetic rate?) was reached. The oxygen excretion was calculated from the radial gradients at various distances from the root tip along individual roots. There seemed to be only minor differences in the excretion rate between newer and older root segments.

3.6.3. Rhizobium Nodules

The nitrogen-fixing enzyme of bacteria, nitrogenase, is denatured by oxygen, and it is therefore only active in microenvironments protected against high oxygen concentrations. The oxygen concentration in the most efficient nitrogen-fixing microenvironment known, the *Rhizobium* nodule, was recently measured with a microelectrode (J. F. Witty, L. Skøt, and N. P. Revsbech, unpublished results). The measurements showed that the oxygen partial pressure within the bacteroid-containing tissue of a pea plant nodule was less than 0.0002 atm. The oxygen gradients through the whole nodule were measured as a function of the external oxygen concentration. The oxygen gradients around the symbiont-containing tissue were extremely steep, with oxygen concentrations dropping from 80% air saturation to 0% within 100 μm. The tissue of the nodule consumed all the incoming oxygen and kept the symbiont-containing region at extremely low oxygen concentrations even when the surrounding atmosphere contained significantly higher oxygen levels than found in nature. Only at an oxygen partial pressure as high as 0.8 atm did the diffusive influx exceed the rate of consumption and cause a breakdown of the oxygen barrier. The oxygen concentration then rose simultaneously in all parts of the symbiont-containing region, suggesting a very efficient transport of oxidizing power by the leghemoglobin in the nodule.

3.6.4. Microbial Films from Sewage Treatment Plants

Microbial films or slimes in sewage treatment plants and similar organic-rich environments may have high microbial activities and consequently also contain steep chemical gradients. The gradients of oxygen associated with such films have been studied over the last decade by H. R. Bungay and coworkers.

It was found that the current velocity, organic load, and pH of the overlying water influenced the oxygen profile in microbial slimes (Bungay *et al.,* 1969; Chen and Bungay, 1981). When the organic load was high,

oxygen penetrated to a very shallow depth (~0.15 mm) due to a high respiratory activity, but the oxygen penetration was considerably deeper when the load was low. A similar effect was observed by J. G. Kuenen (unpublished results). He measured an oxygen penetration of 0.4 mm when the slime was covered with pure water, but only 0.1 mm when the organic load was high. Low pH (<5) inhibited respiratory activity in the film and therefore caused deep oxygen penetrations (Chen and Bungay, 1981). Photosynthetic oxygen production in biofilms containing microalgae caused high oxygen concentrations and deep oxygen penetrations (Bungay and Chen, 1981; Chen and Bungay, 1981). A photosynthetic rate of 56 mmole O_2/m^2 per hr was measured in a photosynthetic biofilm from a trickling filter (J. G. Kuenen, B. B. Jørgensen, and N. P. Revsbech, unpublished data), but ~70% of this oxygen was concurrently consumed within the biofilm. The oxygen consumption of the slime during illumination was several times as high as the rate measured in the dark. During dark incubation, the oxygen consumption of the biofilm was limited by the rate of oxygen diffusion (Chen and Bungay, 1981), and the photosynthetically produced oxygen relieved this limitation.

3.6.5. Epiphytic Communities

Epiphytic communities occur in both freshwater and seawater environments. Oxygen and pH gradients as well as photosynthesis rates have been measured in such communities (Sand-Jensen *et al.*, 1985, and unpublished results). There was no problem in measuring oxygen and pH, but the photosynthetic activity of the epiphytes could not be distinguished from the activity of the macrophyte in layers closer than 0.1–0.2 mm from the macrophyte surface.

Epiphytes and macrophyte often contributed equally to the combined primary production. As an example, a 1.0- to 1.5-mm-thick epiphyte layer on a leaf of the freshwater angiosperm *Potamogeton crispus* was responsible for 70% of the combined primary production of the association (9 mmole O_2/m^2 per hr) when illuminated at 500 μEinst/m^2 per sec. The investigated epiphytic communities were all photosaturated at relatively low light intensities (100–300 μEinst/m^2 per sec). This is in contrast to microalgal photosynthesis in sediments, which is usually not saturated at even very high light intensities (Section 3.2.2c). The light compensation points of the associations were also low, 20–40 μEinst/m^2 per sec. The epiphytes increased the pH values and the oxygen concentrations at the leaf surface as compared to macrophytes without epiphytes, and this may be as significant as the shading effect often mentioned as the major negative effect of epiphytes on the host macrophyte.

3.6.6. The Air–Water Interface

All exchange of gases between atmosphere and water occurs through the air–water interface. The rate of transfer seems to be governed by molecular diffusion through a diffusive boundary layer (Section 3.1.3) immediately below the surface of the water (e.g., Broecker and Peng, 1974). The oxygen gradients within the diffusive boundary layer can be measured using an oxygen microelectrode where the tip is bent into a U-shape, so that the oxygen gradient can be measured upward. The miniscus formed around the electrode shaft due to the surface tension is then formed around the electrode shaft at such a great distance from the point being analyzed that it does not affect the measured gradients. An example of an oxygen profile down through the boundary layer of nonstirred, partly deoxygenated water is shown in Fig. 29. The oxygen gradient was linear down through the diffusive boundary layer, which was about 500 μm in thickness. At greater than 600 μm depth, the concentration gradient was zero, indicating some turbulence even in the absence of stirring.

4. Future Developments

The technical development of gas- and ion-sensing microelectrodes and of the associated equipment is still in an early phase. Over the coming few years one can expect a number of novel microelectrode types to be developed, some of which exist currently as macroelectrodes. The specificity and sensitivity of these electrodes are rapidly improving and the measuring circuits and data handling systems are becoming more advanced, less expensive, and simpler to use. As the electrodes become more widely applied, more microelectrode types should also become

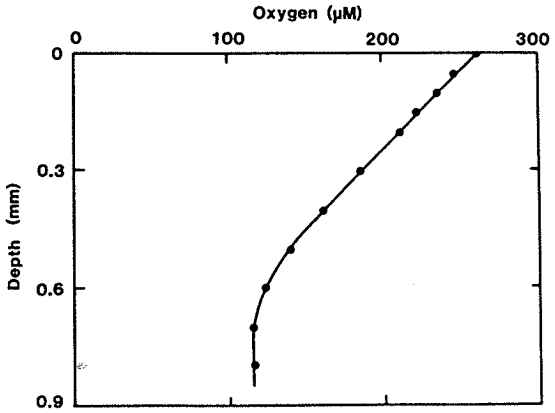

Figure 29. Oxygen profile through the diffusive boundary layer at the air–water interface of a nonstirred column of water. The water was contained in a 100-ml beaker and was partly deoxygenated by N_2-bubbling 15 min before the oxygen profile was recorded. [Data from B. B. Jørgensen and N. P. Revsbech (in preparation).]

commercially available to the occasional user, for whom learning the requisite construction techniques may remain a barrier.

Currently used microelectrodes that should be of interest in microbial ecology besides those sensitive to PO_2, pS^{2-}, and pH, are the CO_2- and Ca^{2+}-sensitive types. Both have been developed to a stage where they can be applied to many microbial systems (Caflish and Carter, 1974; Pucacco and Carter, 1978; Thomas, 1978; Tsien, 1980). The CO_2 microelectrode can be used, as can the O_2 electrode, to analyze respiration and photosynthesis of microorganisms. A disadvantage of the CO_2 microelectrode for photosynthesis studies, however, is, that this process is generally accompanied by high pH, at which little CO_2 is present, and the applicability therefore may be limited due to insufficient sensitivity. Carbonate-sensitive liquid membrane electrodes have also been constructed (Herman and Rechnitz, 1975), but they still have problems of interference from other common ions, which make them impractical for most ecological applications. Calcium-sensitive microelectrodes have important potential applications in the study of calcification and carbonate dissolution.

Many new liquid ion exchangers are developed each year and some are sufficiently specific to be used as membranes in ion-sensitive microelectrodes (Tsien, 1980). Such ion exchangers have already been used in microelectrodes for pH, Na^+, K^+, and Ca^{2+}. In addition, an ammonia-sensitive, potentiometric microprobe has been developed (Pui *et al.*, 1978). A quite different principle is used in the voltammetric microelectrodes that have recently been fabricated with sensing tips of less than 10 μm diameter (Wightman, 1981; Howell and Wightman, 1984). Although these electrodes may not be ideal for many applications, due to problems with their specificity, they can be used to detect a wide range of chemical species in solution.

Novel types of sensors presently being developed as macroelectrodes are based on specific enzyme reactions. Immobilized enzymes at the electrode tip react with specific organic molecules in the surrounding medium and create an electrochemical reaction, which can be recorded. An electrode that responds to, for example, glucose has been constructed according to this principle (Tsuchida and Yoda, 1981). Such electrodes may have a high specificity toward the reacting organic molecules as a result of the high specificity of the enzymatic reactions. In the near future it may be possible to scale down such electrodes to real microscale and make them important new tools for the study of metabolic processes in natural microbial communities. Enzyme-reactive sensors are also being developed based on light detection rather than electrochemical detection (Arnold, 1985). By the use of single optical fibers as light guides, it should be possible to apply similar principles on the microscale.

In addition to the appearance of new types of sensors, the performance of available microelectrodes and measuring equipment is being refined. The new microprocessor technology has made data collection and handling much faster, better, and, at least in some respects, also simpler. For, example, microprocessors can be used to compensate for slow response times of the microelectrodes and for drift in the signal. Electronic compensation for slow response can be especially useful in combination with continuously moving microelectrodes operated by a motor-driven micromanipulator. Semiconductor technology has also provided inexpensive operational amplifiers small enough to attach directly to the microelectrodes, thereby improving the signal-to-noise ratio. Such amplifiers provide more stability and flexibility, especially when operating the microelectrodes in the field, on board a ship, or by remote control.

The introduction and application of microelectrodes in ecological research has invariably led to the wish for additional microsensors. These should measure environmental parameters such as light, temperature, and salinity at a spatial resolution sufficiently high to be directly relevant to the individual microbial populations. Such sensors are also slowly being developed. As one example, a simple light sensor has recently been constructed with a tip diameter of 20–30 μm (B. B. Jørgensen and D. J. Des Marais, in preparation). The probe is based on a single optical fiber of 80 μm diameter with a conical sensing tip. The applied semiconductor detector is a hybrid photodiode/amplifier and the complete unit is directly attached to a micromanipulator, just like a microelectrode.

The range of microbial environments so far studied and the ecological research applications of microelectrodes are still quite limited. For many basic problems and applied aspects of microbial ecology, the use of microelectrodes seems an ideal but yet unexplored possibility. Bacteria often grow on surfaces or at interfaces within a chemical microenvironment quite different from the surrounding medium. These chemical conditions are difficult to analyze with other currently available techniques. Thus, microelectrodes have important future applications in the study of, e.g, the corrosion of off-shore steel constructions, oil degradation in the sea, the develpoment of bacterial plaque on teeth, and the metabolism of immobilized bacterial films in biotechnology.

References

Alexander, M., 1977, *Introduction to Soil Microbiology,* Wiley, New York.

Aller, R. C., 1977, The Influence of Macrobenthos on Chemical Diagenesis of Marine Sediments, Ph.D. thesis, Yale University.

Ammann, D., Lanter, F., Steiner, R. A., Schultess, P., Shijo, Y., and Simon, W., 1981, Neu-

tral carrier based hydrogen ion selective microelectrode for extra- and intracellular studies, *Anal. Chem.* **53**:2267–2269.

Anderson, O. R., and Be, A. W. H., 1976, The ultrastructure of a planktonic foraminifer, *Globigerinoides sacculifer* (Brady), and its symbiotic dinoflagellates, *J. Foram. Res.* **6**:1–21.

Armstrong, W., 1967, The use of polarography in the assay of oxygen diffusing from roots in anaerobic media, *Physiol. Plant.* **20**:540–553.

Arnold, M. A., 1985, Enzyme-based fiber optic sensor, *Anal. Chem.* **57**:565–566.

Baumgärtl, H., and D. W. Lübbers, 1983, Platinum needle electrodes for polarographic measurement of local O_2 pressure in cellular range of living tissue. Its construction and properties, in: *Polarographic Oxygen Sensors: Aquatic and Physiological Applications* (E. Gnaiger and H. Forstner, eds.), pp. 37–65, Springer-Verlage, Heidelberg.

Be, A. W. H., and Tolderlund, D. S., 1971, Distribution and ecology of living planktonic foraminifera in surface waters of the Atlantic and Indian Oceans, in: *Micropaleontology of Oceans* (B. M. Funnell and W. R. Riedel, eds.), pp. 105–149, Cambridge University Press, Cambridge.

Berner, R. A., 1962, Electrode studies of hydrogen sulfide in marine sediments, *Geochim. Cosmochim. Acta* **27**:563–575.

Berner, R. A., 1980, *Early Diagenesis, a Theoretical Approach,* Princeton University Press, Princeton, New Jersey.

Board, P. A., 1976, Anaerobic regulation of atmospheric oxygen, *Atmos. Environ.* **10**:339–342.

Boudreau, B. P., and Guinasso, N. L., 1982, The influence of a diffusive boundary sublayer on accretion, dissolution, and diagenesis at the sea floor, in: *The Dynamic Environment of the Sea Floor* (K. A. Fanning and F. T. Manheim, eds.), pp. 115–145, Lexington Books, Lexington, Massachusetts.

Broecker, W. S., and Peng, T.-H, 1974, Gas exchange rate between sea and air, *Tellus* **26**:21–35.

Bungay, H. R., and Chen, Y. S., 1981, Dissolved oxygen profiles in photosynthetic microbial slimes, *Biotechnol. Bioeng.* **23**:1893–1895.

Bungay, H. R., 3rd, Whalen, W. J., and Sanders, W. M., 1969, Microprobe techniques for determining diffusivities and respiration in microbial slime systems, *Biotechnol. Bioeng.* **11**:765–772.

Caflish, C. R., and Carter, N. W., 1974, A micro PCO_2 electrode, *Anal. Biochem.* **60**:252–257.

Chen, Y. S., and Bungay, H. R., 1981, Microelectrode studies of oxygen transfer in trickling filter slimes, *Biotechnol. Bioeng.* **23**:781–792.

Clark, L. C., Wolf, R., Granger, D., and Taylor, A., 1953, Continuous recording of blood oxygen tension by polarography, *J. Appl. Physiol.* **6**:189–193.

Cohen, Y., 1983, The Solar Lake cyanobacterial mats: Strategies of photosynthetic life under sulfide, in: *Microbial Mats: Stromatolites* (Y. Cohen, R. W. Castenholz, and H. O. Halvorson, eds.), pp. 133–148, Alan R. Liss, New York.

Cohen, Y., Padan, E., and Shilo, M., 1975a, Facultative anoxygenic photosynthesis in the cyanobacterium *Oscillatoria limnetica, J. Bacteriol.* **123**:855–861.

Cohen, Y., Jørgensen, B. B., Padan, E., and Shilo, M., 1975b, Sulfide dependent anoxygenic photosynthesis in the cyanobacterium *Oscillatoria limnetica, Nature* **257**:489–492.

Crank, J., 1983, *The Mathematics of Diffusion,* Oxford University Press, London.

Dale, T., 1978, Total, chemical, and biological oxygen consumption of the sediments in Lindåspollene, Western Norway, *Mar. Biol.* **49**:333–341.

Davis, R. B., 1974, Tubificids alter profiles of redox potential and pH in profundal lake sediment, *Limnol. Oceanogr.* **19**:342–346.

Drew, E. A., 1973, The biology and physiology of alga–invertebrate symbioses. III *In situ* measurements of photosynthesis and calcification in some hermatypic corals, *J. Exp. Mar. Biol. Ecol.* **13**:165–179.

Duursma, E. K., and Hoede, C., 1967, Theoretical, experimental and field studies concerning molecular diffusion of radioisotopes in sediments and suspended solid particles of the sea. Part A: Theories and mathematical calculations, *Neth. J. Sea Res.* **3**:423–457.

Edwards, R. W., 1958, The effect of larvae of *Chironemus riparius* Meigen on the redox potentials of settled activated sludge, *Ann. Appl. Biol.*. **46**:457–464.

Fenchel, T., 1969, The ecology of marine microbenthos. 4. Structure and function of the benthic ecosystem, its chemical and physical factors and the meiofauna communities with special reference to the ciliated protozoa, *Ophelia* **6**:1–182.

Fluhler, H., Ardakan, M. S., Szusckiewicz, and Stolzy, L. H., 1976, Field measured nitrous oxide concentrations, redox potentials, oxygen diffusion rates, and oxygen partial pressures in relation to denitrification, *Soil Sci.* **122**:107–114.

Greenwood, D. J., and Goodman, D., 1967, Direct measurement of the distribution of oxygen in soil aggregates and in columns of fine soil crumbs, *J. Soil. Sci.* **18**:182–196.

Guterman, H., and Ben-Yaakov, S., 1983, Determination of total dissolved sulfide in the pH range 7.5 to 11.5 by ion selective electrodes, *Anal. Chem.* **55**:1731–1734.

Harris, G. P., 1978, Photosynthesis, productivity and growth: The physiological ecology of phytoplankton, *Ergeb. Limnol.* **10**:1–171.

Herman, H. B., and Rechnitz, G. A., 1975, Preparation and properties of a carbonate ion-selective membrane electrode, *Anal. Chim. Acta* **76**:155–164.

Howell, J. O., and Wightman, R. M., 1984, Ultrafast voltammetry and voltammetry in highly resistive solutions with microvoltammetric electrodes, *Anal. Chem.* **56**:524–529.

Hunding, C. and Hargrave, B. T., 1973, A comparison of benthic microalgal production measured by C^{14} and oxygen methods, *J. Fish. Res. Board Can.* **30**:309–312.

Jerlov, N., 1976, *Optical Oceanography,* Elsevier, Amsterdam.

Jones, J. G., Gardener, S., and Simon, B. M., 1983, Bacterial reduction of ferric iron in stratified lake, *J. Gen. Microbiol.* **129**:131–139.

Jørgensen, B. B., 1977, The sulfur cycle of a coastal marine sediment (Limfjorden, Denmark), *Limnol. Oceanogr.* **22**:814–832.

Jørgensen, B. B., 1982, Ecology of the bacteria of the sulfur cycle with special reference to anoxic–oxic interface environments, *Phil. Trans. R. Soc. Lond. B* **298**:543–561.

Jørgensen, B. B., 1983, The microbial sulfur cycle, in: *Microbial Geochemistry* (W. E. Krumbein, ed.), pp. 91–124, Blackwell, Oxford.

Jørgensen, B. B., and Revsbech, N. P., 1983, Colorless sulfur bacteria, *Beggiatoa* spp. and *Thiovolum* spp. in O_2 and H_2S microgradients, *Appl. Environ. Microbiol.* **45**:1261–1270.

Jørgensen, B. B., and Revsbech, N. P., 1985, Diffusive boundary layers and the oxygen uptake of sediments and detritus, *Limnol. Oceanogr.* **30**:11–21.

Jørgensen, B. B., Revsbech, N. P., Blackburn, T. H., and Cohen, Y., 1979, Diurnal cycle of oxygen and sulfide microgradients and microbial photosynthesis in a cyanobacterial mat sediment, *Appl. Environ. Microbiol.* **38**:46–58.

Jørgensen, B. B., Revsbech, N. P., and Cohen, Y., 1983, Photosynthesis and structure of benthic microbial mats: Microelectrode and SEM studies of four cyanobacterial communities, *Limnol. Oceanogr.* **28**:1075–1093.

Jørgensen, B. B., Erez, J., Revsbech, N. P., and Cohen, Y., 1985, Symbiotic photosynthesis in planktonic foraminifera, *Globigerinoides sacculifer* (Brady), studied with microelectrodes, *Limnol. Oceanogr.* **30**:1253–1267.

Jørgensen, B. B., Cohen, Y., and Revsbech, N. P., 1986, Transition from anoxygenic to oxygenic photosynthesis in a microcoleus chtonoplastes Cyanobacterial mat, *Appl. Environ. Microbiol.* **51** (2) (in press).

Joshi, M. M., and Hollis, J. P., 1977, Interaction of *Beggiatoa* and rice plant: Detoxification of hydrogen sulfide in the rice rhizosphere, *Science* **195**:179–180.

Kelly, D. P., 1982, Biogeochemistry of the chemolithotrophic oxidation of inorganic sulfur, *Phil. Trans. R. Soc. Lond. B* **298**:499–528.

Lean, D. R. S., and Burnison, B. K., 1979, An evaluation of errors in the ^{14}C method of primary production measurement, *Limnol. Oceanogr.* **24**:917–928.

Lemon, E. R., and Erickson, A. E., 1952, The measurement of oxygen diffusion in soil with a platinum microelectrode, *Soil Sci. Soc. Am. Proc.* **16**:160–163.

Lindeboom, H. J., and Sandee, A. J. J., 1984, The effect of coastal engineering projects on microgradients and mineralization reactions in sediments, *Water Sci. Technol.* **16**:87–94.

Murray, J. W., and Grundmanis, V., 1980, Oxygen consumption in pelagic marine sediments, *Science* **209**:1527–1530.

Naylor, P. F. D., and Evans, N. T. S., 1960, An electrode for measuring absolute oxygen tension in tissues, *J. Polarogr. Soc.* **2**:22–24.

Nelson, D. C., and Jannasch, H. W., 1983, Chemoautotrophic growth of a marine *Beggiatoa* in sulfide-gradient cultures, *Arch. Microbiol.* **136**:262–269.

Pamatmat, M. M., 1971, Oxygen consumption by the seabed. IV Shipboard and laboratory experiments, *Limnol. Oceanogr.* **16**:536–550.

Prezelin, B. B., 1976, The role of peridinin-chlorophyll a-protein in the photosynthetic light adaptation of the marine dinoflagellate, *Glenodinium* sp., *Planta* **130**:225–233.

Prezelin, B. B., Ley, A. C., and Haxo, F. T., 1976, Effects of growth irradiance on the photosynthetic action spectra of the marine dinoflagellate, *Glenodinium* sp., *Planta* **130**:251–256.

Pucacco, L. R., and Carter, N. W., 1978, An improved PCO_2 microelectrode, *Anal. Biochem.* **90**:427–434.

Pui, C. P., Rechnitz, G. A., and Miller, R. F., 1978, Micro-size potentiometric probes for gas and substrate sensing, *Anal. Chem.* **50**:330–333.

Purcell, E. M., 1977, Life at low Reynolds number, *Am. J. Phys.* **45**(1):3–11.

Reimers, C. E., and Smith, K. L., 1986, Reconciling measured and predicted fluxes of oxygen across the deep sea sediment–water interface, *Limnol. Oceanogr.*

Reimers, C. E., Kalhorn, S., Emerson, S. R., and Nealson, K. H., 1984, Oxygen consumption rates in pelagic sediments from the Central Pacific: First estimates from microelectrode profiles, *Geochim. Cosmochim. Acta* **48**:903–911.

Revsbech, N. P., 1983, *In situ* measurement of oxygen profiles of sediments by use of oxygen microelectrodes, in: *Polarographic Oxygen Sensors: Aquatic and Physiological Applications* (E. Gnaiger and H. Forstner, eds.), pp. 265–273, Springer, Heidelberg.

Revsbech, N. P., and Jørgensen, B. B., 1983, Photosynthesis of benthic microflora measured with high spatial resolution by the oxygen microprofile method: Capabilities and limitations of the method, *Limnol. Oceanogr.* **28**:749–756.

Revsbech, N. P., and Ward, D. M., 1983, Oxygen microelectrode that is insensitive to medium chemical composition: Use in an acid microbial mat dominated by *Cyanidium caldarium, Appl. Environ. Microbiol.* **45**:755–759.

Revsbech, N. P., and Ward, D. M., 1984a, Microprofiles of dissolved substances and photosynthesis in microbial mats measured with microelectrodes, in: *Microbial Mats: Stromatolites* (Y. Cohen, R. W. Castenholz, and H. O. Halvorson, eds.), pp. 171–188, Alan R. Liss, New York.

Revsbech, N. P., and Ward, D. M., 1984b, Microelectrode studies of interstitial water chemistry and photosynthetic activity in a hot spring microbial mat, *Appl. Environ. Microbiol.* **48**:270–275.

Revsbech, N. P., Jørgensen, B. B., and Blackburn, T. H., 1980a, Oxygen in the seabottom measured with a microelectrode, *Science* **207**:1355–1356.

Revsbech, N. P., Sørensen, J., Blackburn, T. H., and Lomholt, J. P., 1980b, Distribution of oxygen in marine sediments measured with microelectrodes, *Limnol. Oceanogr.* **25**:403–411.

Revsbech, N. P., Jørgensen, B. B., and Brix, O., 1981, Primary production of microalgae in sediments measured by oxygen microprofile, $H^{14}CO_3^-$ fixation and oxygen exchange methods, *Limnol. Oceanogr.* **26**:717–730.

Revsbech, N. P., Jørgensen, B. B., Blackburn, T. H., and Cohen, Y., 1983, Microelectrode studies of photosynthesis and O_2, H_2S, and pH profiles of a microbial mat, *Limnol. Oceanogr.* **28**:1062–1074.

Revsbech, N. P., Madsen, B., and Jørgensen, B. B., 1986, Oxygen production and consumption in sediments determined at high spatial resolution by computer simulation of oxygen microelectrode data, *Limnol. Oceanogr.* (in press).

Sand-Jensen, K., Prahl, C., and Stockholm, H., 1982, Oxygen release from roots of submerged aquatic macrophytes, *Oikos* **38**:349–354.

Sand-Jensen, K., Revsbech, N. P., and Jørgensen, B. B., 1985, Microprofiles of oxygen in epiphyte communities on submerged macrophytes, *Mar. Biol.* **89**:55–62.

Santschi, P. H., Bower, P., Nyffeler, U. P., Azvedo, A., and Broecker, W. S., 1983, Estimates of the resistance of chemical transport posed by the deep-sea boundary layer, *Limnol. Oceanogr.* **28**:899–912.

Sexstone, A. J., Revsbech, N. P., Parkin, T. B., and Tiedje, J. M., 1985, Direct measurement of oxygen profiles and denitrification rates in soil aggregates, *Soil Sci. Soc. Am. J.* **49**:645–651.

Shiver, D. F., 1969, *The Manipulation of Air-Sensitive Compounds,* McGraw-Hill, New York.

Smith, K. L., Jr., and Baldwin, R. J., 1984, Seasonal fluctuation in deep-sea sediment community respiration: Central and eastern North Pacific, *Nature* **307**:624–626.

Smith, K. L., Jr., and Hinga, K. R., 1983, Sediment community respiration in the deep sea, in: *The Sea* (G. T. Rowe, ed.), Vol. 8, pp. 331–370, Wiley, New York.

Sørensen, J., 1984, A headspace technique for oxygen measurement in deep-sea sediment cores, *Limnol. Oceanogr.* **29**:650–652.

Sørensen, J., Jørgensen, B. B., and Revsbech, N. P., 1979, A comparison of oxygen, nitrate, and sulfate respiration in coastal marine sediments, *Microb. Ecol.* **5**:105–115.

Stanier, R. Y., Adelberg, E. A., and Ingraham, J. L., 1977, *General Microbiology,* 4th ed., Macmillan, London.

Steemann-Nielsen, E., 1952, Use of radioactive carbon (C^{14}) for measuring organic production in the sea, *J. Cons. Cons. Int. Explor. Mer* **18**:117–140.

Thomas, R. C., 1978, *Ion-Sensitive Intracellular Microelectrodes, How to Make and Use Them,* Academic Press, London.

Tsien, R. Y., 1980, Liquid sensors for ion-selective microelectrodes. *Trends Neurosci.* **3**:219–221.

Tsuchida, T., and Yoda, K., 1981, Immobilization of D-glucose oxidase onto a hydrogen peroxide permselective membrane and application for an enzyme electrode, *Enzyme Microb. Technol.* **3**:326–330.

Vogel, S., 1981, *Life in Moving Fluids,* Willard Grant, Boston.

Ward, D. M., Beck, E., Revsbech, N. P., Sandbeck, K. A., and Winfrey, M. R., 1984, Decomposition of hot spring microbial mats, in: *Microbial Mats: Stromatolites* (Y. Cohen, R. W. Castenholz, and H. O. Halvorson, eds.), pp. 191–214, Alan R. Liss, New York.

Whalen, W. J., Riley, J., and Nair, P., 1967, A microelectrode for measuring intracellular PO_2, *J. Appl. Physiol.* **23**:798–801.

Wightman, R. M., 1981, Microvoltammetric electrodes, *Anal. Chem.* **53**:1125A–1130A.

Wimbush, M., 1976, The physics of the benthic boundary layer, in: *The Benthic Boundary Layer* (I. N. McCave, ed.), pp. 3–10, Plenum Press, New York.